Semilocal Density Functionals for Exchange and Correlation: Theory and Applications

Kieron Burke, John P. Perdew, and Mel Levy

Quantum Theory Group, Tulane University, New Orleans, LA 70118

Advances in our understanding of density functionals have led to the Perdew-Wang 91 (PW91) generalized gradient approximation (GGA), a nonempirical semilocal functional which shows systematic improvement on the local spin density (LSD) approximation. In this article, we discuss some exact conditions satisfied by all electronic systems, including hole and coordinate-scaling requirements, and we discuss which of these the LSD approximation obeys. To illustrate our points, we invoke Hooke's atom, an analytically solvable two-electron system. We then discuss the history of GGA's, which satisfy many conditions that the LSD approximation gets right, plus others. We also make a graphical comparison of the gradient dependence of various GGA's, concluding that PW91 has the best formal properties. Since the construction of PW91, we have made further progress in the study of exact conditions satisfied by all electronic systems, and we give a review of some of the results. The recently-discovered low-density convexity constraint provides a difficult challenge for approximate functionals to satisfy. We conclude with a survey of recent applications of GGA's to atoms, molecules, clusters, surfaces, and solids.

1. INTRODUCTION

In this section, we discuss first the basic formalism of density functional theory, and the Kohn-Sham equations whose solution yields the ground state density and energy of a system. We next describe a two-electron system, called Hooke's atom, which has the highly unusual feature of an *analytic* ground state, and is therefore of considerable pedagogical value. Lastly we discuss the notation and organization of this article.

1.1. The Kohn-Sham equations

The problem of finding the ground-state properties of a system of $N(> 1)$ electrons is important in the study of atoms, molecules, clusters, surfaces, and solids. Since no exact solution exists in general, many approximate methods have been developed for approaching this problem. Each successful method has its own advantages and disadvantages.

Wavefunction methods[1] have proved very successful in the study of small molecules. They have the important merit that their accuracy can be systematically improved by enlarging the size of the calculation. Unfortunately, since

their implementation implies finding the wavefunction, which depends on $3N$ coordinates, for large N they become prohibitively expensive in terms of computer time/memory. Hence their success for molecules, and inapplicability to solids.

The density, on the other hand, is a function of only 3 spatial variables, $\mathrm{r} = x, y, z$, so it is a much easier quantity to work with in practice. Furthermore, the ground-breaking work of Hohenberg and Kohn[2], and its subsequent extension in the constrained search formulation[3–5] proved that all quantities of interest could, in principle, be determined from knowledge of the density alone.

The basic idea in density functional theory is to replace the Schrödinger equation for the interacting electronic system with a set of single-particle equations whose density is the same as that of the original system. These equations are the Kohn-Sham equations[6], and may be written

$$\left[-\frac{1}{2}\nabla^2 + v_\sigma(\mathrm{r}) + \int d^3 r' \frac{n(\mathrm{r}')}{|\mathrm{r} - \mathrm{r}'|} + v_{xc,\sigma}([n_\uparrow, n_\downarrow]; \mathrm{r}) \right] \psi_{\alpha,\sigma}(\mathrm{r}) = \epsilon_{\alpha,\sigma} \, \psi_{\alpha,\sigma}(\mathrm{r}). \tag{1}$$

where $\sigma = \uparrow$ or $\downarrow$ is the spin index, α labels the Kohn-Sham orbitals, $v_\sigma(\mathrm{r})$ is the (spin-dependent) external potential, and $v_{xc,\sigma}([n_\uparrow, n_\downarrow]; \mathrm{r})$ is the exchange-correlation potential, defined below, which is a functional of the spin densities. The total density of the system is then

$$n(\mathrm{r}) = n_\uparrow(\mathrm{r}) + n_\downarrow(\mathrm{r}), \tag{2}$$

where

$$n_\sigma(\mathrm{r}) = \sum_\alpha |\psi_{\alpha,\sigma}(\mathrm{r})|^2 \theta(\mu - \epsilon_{\alpha,\sigma}). \tag{3}$$

The sum in Eq. (3) is over all Kohn-Sham orbitals, and μ is the chemical potential. The total ground state energy is

$$\begin{aligned} E &= \sum_{\alpha,\sigma} \langle \psi_{\alpha,\sigma} | - \frac{1}{2}\nabla^2 | \psi_{\alpha,\sigma} \rangle \theta(\mu - \epsilon_{\alpha,\sigma}) + \sum_\sigma \int d^3 r \; n_\sigma(\mathrm{r}) \, v_\sigma(\mathrm{r}) \\ &\quad + \frac{1}{2} \int d^3 r \int d^3 r' \frac{n(\mathrm{r}) \, n(\mathrm{r}')}{|\mathrm{r} - \mathrm{r}'|} + E_{xc}[n_\uparrow, n_\downarrow] \end{aligned} \tag{4}$$

where $E_{xc}[n_\uparrow, n_\downarrow]$ is the exchange-correlation energy of the system, in terms of which $v_{xc,\sigma}(\mathrm{r}) = \delta E_{xc}/\delta n_\sigma(\mathrm{r})$.

These equations are exact for any electronic system, if the *exact* functional $E_{xc}[n_\uparrow, n_\downarrow]$ is used. Unfortunately, it is impossible to know this functional exactly for most systems, and approximations need to be made to apply these equations to real systems. However, once such an approximation is made, the resulting equations are straightforward to solve, being a set of self-consistent equations for the orbitals $\psi_{\alpha,\sigma}(\mathrm{r})$. The remainder of this article is devoted to how such approximations are constructed, and how well they perform.

Because density functional theory deals directly with the density, and never produces an interacting wavefunction, it has no particular difficulties with large periodic systems. Thus it is the method of choice for solid systems, which contain

$O(10^{23})$ electrons. On the other hand, the functional $E_{xc}[n_\uparrow, n_\downarrow]$ is an extremely sophisticated many-body object, so that robust moderate-accuracy methods (such as the LSD approximation) can be difficult to improve systematically.

We also point out that the Kohn-Sham orbitals bear no known simple relation to the single-particle states of the interacting system. In spite of this, in calculations of the electronic structure of solids, these orbitals are often identified with the quasiparticle states. However, progress in understanding their meaning is being made through the extension of density functional theory to time-dependent external potentials, which can then be applied in the linear response regime[7].

1.2. Hooke's atom

It is not easy to find a quantum many-body system for which the Schrödinger equation may be solved analytically. However, a useful example is provided by the problem of two electrons in an external harmonic-oscillator potential, called Hooke's atom. The Hamiltonian for this system is

$$H = -\frac{1}{2}\left(\nabla_1^2 + \nabla_2^2\right) + \frac{1}{2}k(r_1^2 + r_2^2) + \frac{1}{|\mathbf{r}_2 - \mathbf{r}_1|} \tag{5}$$

where $\nabla_i = \partial/\partial \mathbf{r}_i$. In center-of-mass and relative coordinates, this becomes

$$H = -\left(\frac{1}{4}\nabla_\mathbf{R}^2 + \nabla_\mathbf{u}^2\right) + kR^2 + \frac{k}{4}u^2 + \frac{1}{u} \tag{6}$$

where $\mathbf{R} = (\mathbf{r}_1 + \mathbf{r}_2)/2$ and $\mathbf{u} = \mathbf{r}_2 - \mathbf{r}_1$. For spin singlet states, the total wavefunction may therefore be separated:

$$\Psi(\mathbf{r}_1 s_1, \mathbf{r}_2 s_2) = \varphi(\mathbf{u})\, \xi(\mathbf{R})\, \chi(s_1, s_2) \tag{7}$$

where $\chi(s_1, s_2)$ is the singlet spin wavefunction. The motion in $\mathbf{R}$ is simply that of a three-dimensional harmonic oscillator with mass 2 and force constant $2k$. For the motion in $\mathbf{u}$, we can separate the angular and radial contributions as

$$\varphi(\mathbf{u}) = \frac{f(u)}{u} Y_{lm}(\Omega_u). \tag{8}$$

From Eq. (6), this yields a second-order differential equation for the interelectronic function $f(u)$, namely

$$\left[-\frac{1}{2}\frac{d^2}{du^2} + \frac{1}{8}\omega^2 u^2 + \frac{1}{2u} + \frac{l(l+1)}{2u^2}\right] f(u) = \frac{\epsilon}{2} f(u), \tag{9}$$

where $\omega = \sqrt{k}$ is the oscillator frequency and ϵ is the contribution to the total energy due to the relative motion of the electrons.

For any value of the force constant k, at most a single differential equation needs to be solved to find the ground state of this system. This has been done numerically[8] for many values of k. More recently, Kais[9] and co-workers have studied the special case of $k = 1/4$, for which an analytic solution exists, while Taut has shown that analytic solutions exist for an infinite, discrete set of oscillator

frequencies, including both ground and excited states[10]. Those corresponding to extremely low densities have been studied in some detail[11].

Throughout this paper, we use Hooke's atom to illustrate our points. We often use results calculated for the $k = 1/4$ case, for which the exact density is plotted in Figure 1. We think of this as a sort of "poor man's Helium," although we note
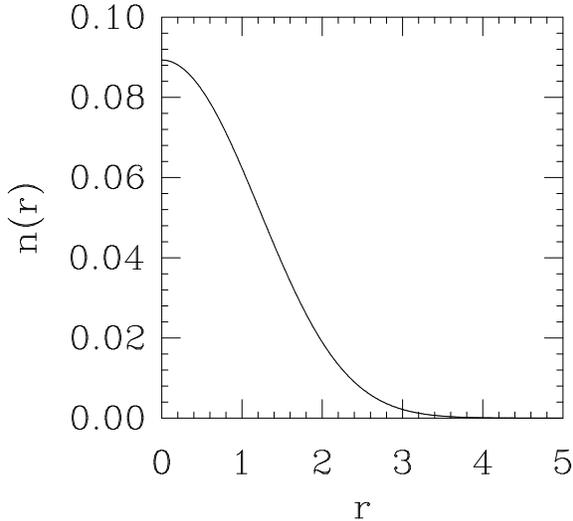

Figure 1. Ground state density of Hooke's atom for $k = 1/4$.

several qualitative differences from real He, i.e., no cusp in the density at the origin, and no continuum of unoccupied states above the bound states. These differences are unimportant for the present purposes.

1.3. Notation and organization

We conclude this section with a discussion of our notation. We use atomic units throughout this paper, in which $e^2 = \hbar = m_e = 1$, so that all energies are in Hartrees (27.21 eV) and all distances in Bohr radii (0.529 Å), unless explicitly stated otherwise. We also discuss coupling constant averages, in which the strength of the Coulomb repulsion is given by λe^2, where $0 \leq \lambda \leq 1$, and in which the external potential varies with λ, $v_{\sigma,\lambda}(\mathbf{r})$, in such a way as to keep the spin densities $n_\sigma(\mathbf{r})$ fixed[12]. When no notation explicitly indicates otherwise, all quantities are interpreted as having their value at full coupling strength, $\lambda = 1$. When we wish to indicate the λ dependence of a quantity, we use a subscript λ. Finally, when we consider the coupling-constant average of some quantity, we use an overline. For example, for the pair distribution function defined in the next section, $g(\mathbf{r}', \mathbf{r})$ denotes its value

for $\lambda = 1$, $g_\lambda(\mathbf{r}', \mathbf{r})$ denotes its value as a function of λ, and $\bar{g}(\mathbf{r}', \mathbf{r}) = \int_0^1 d\lambda \; g_\lambda(\mathbf{r}', \mathbf{r})$. The sole exception to this rule is in the exchange-correlation energy itself. As we show in section 2.1, it can be considered as a coupling-constant averaged quantity. We nevertheless keep the traditional notation of E_{xc}, i.e., without a bar.

This article is organized as follows. Section 2 is a discussion of many conditions which all electronic systems are known to satisfy. Section 3 is a discussion of the LSD approximation and semilocal functionals. Section 4 describes some recent progress made in the study of exact conditions, while section 5 describes results of recent applications of GGA's in real physical and chemical systems.

2. SOME EXACT CONDITIONS SATISFIED BY ALL ELECTRONIC SYSTEMS

In this section, we discuss some of the many exact conditions that can be shown to be satisfied by *all* interacting electronic systems in their ground states. We look at both real space and momentum space decompositions of the exchange-correlation energy. In the following sections, we show how knowledge of these exact conditions has been vital to the construction and testing of approximate density functionals.

2.1. Exchange-correlation hole

We begin with some exact conditions on E_{xc} based on its real space decomposition. We define the second order density matrix in terms of the wavefunction

$$\rho_2(\mathbf{r}\sigma, \mathbf{r}'\sigma') = N(N-1) \sum_{\sigma_3,...,\sigma_N} \int d^3 r_3 ... \int d^3 r_N \left| \Psi(\mathbf{r}\sigma, \mathbf{r}'\sigma', ..., \mathbf{r}_N \sigma_N) \right|^2, \qquad (10)$$

where Ψ is the many-body wavefunction. (Note that this definition differs from that of Ref.[13] by a factor of 2.) This function has the probability interpretation that $\rho_2(\mathbf{r}\sigma, \mathbf{r}'\sigma') \; d^3 r \; d^3 r'$ is the probability of finding an electron of spin σ in volume element $d^3 r$ at $\mathbf{r}$ and another electron of spin σ' in volume element $d^3 r'$ at $\mathbf{r}'$. We may define a conditional probability density by

$$\rho_2(\mathbf{r}\sigma, \mathbf{r}'\sigma') \equiv n_\sigma(\mathbf{r}) \; n_2(\mathbf{r}\sigma, \mathbf{r}'\sigma'), \qquad (11)$$

so that $n_2(\mathbf{r}\sigma, \mathbf{r}'\sigma') \; d^3 r'$ is the probability of finding an electron of spin σ' in volume element $d^3 r'$ at $\mathbf{r}'$, given that there is an electron of spin σ in volume element $d^3 r$ at $\mathbf{r}$. The (unaveraged) spin-decomposed exchange-correlation hole around an electron of spin σ at $\mathbf{r}$ is then defined by the relation

$$n_2(\mathbf{r}\sigma, \mathbf{r}'\sigma') \equiv n_{\sigma'}(\mathbf{r}') + n_{xc}(\mathbf{r}\sigma, \mathbf{r}'\sigma'), \qquad (12)$$

while the non-spin decomposed hole is defined as

$$n_{xc}(\mathbf{r}, \mathbf{r}') = \sum_{\sigma,\sigma'} \frac{n_\sigma(\mathbf{r})}{n(\mathbf{r})} n_{xc}(\mathbf{r}\sigma, \mathbf{r}'\sigma'), \qquad (13)$$

so that it is related to the spin-summed second order density matrix by

$$\rho_2(\mathbf{r}, \mathbf{r}') \equiv \sum_{\sigma,\sigma'} \rho_2(\mathbf{r}\sigma, \mathbf{r}'\sigma') = n(\mathbf{r})[n(\mathbf{r}') + n_{xc}(\mathbf{r}, \mathbf{r}')]. \qquad (14)$$

We can further decompose the hole into exchange and correlation contributions:

$$n_{xc}(\mathbf{r}\sigma, \mathbf{r}'\sigma') = n_x(\mathbf{r}\sigma, \mathbf{r}'\sigma') + n_c(\mathbf{r}\sigma, \mathbf{r}'\sigma'). \tag{15}$$

By exchange, we mean the density functional definition of exchange, in which the wavefunction is a Slater determinant whose density is the exact density of the interacting system, and which minimizes the energy of the non-interacting system in the Kohn-Sham external potential, $v_{\sigma,\lambda=0}$. Another useful concept is the pair distribution function, defined as[14]

$$g(\mathbf{r}\sigma, \mathbf{r}'\sigma') = \rho_2(\mathbf{r}\sigma, \mathbf{r}'\sigma')/[n_\sigma(\mathbf{r})n_{\sigma'}(\mathbf{r}')]. \tag{16}$$

The exchange-correlation hole may be written in terms of the pair distribution as

$$n_{xc}(\mathbf{r}\sigma, \mathbf{r}'\sigma') = n_{\sigma'}(\mathbf{r}') \left[g(\mathbf{r}\sigma, \mathbf{r}'\sigma') - 1\right]. \tag{17}$$

Figure 2 is a plot of the exact hole (and its LSD approximation) for the Hooke's atom discussed in section 1.2. The figure is plotted for $k = 1/4$, $\lambda = 1$, and $\mathbf{r} = 0$.
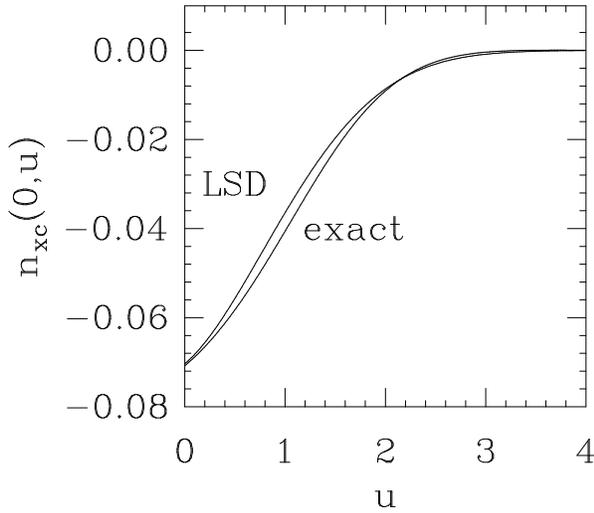

Figure 2. Exchange-correlation hole around an electron at the origin of Hooke's atom.

The exchange-correlation hole is of considerable interest in density functional theory, as the exact exchange-correlation energy may be expressed in terms of this hole. By use of the Hellmann-Feynman theorem, one may write the exchange-correlation energy as the electrostatic interaction between the density and the hole, averaged over coupling constant[13], i.e.,

$$E_{xc} = \int_0^1 d\lambda \, E_{xc,\lambda}[n] = \frac{1}{2} \int d^3r \, n(\mathbf{r}) \int d^3u \, \frac{\bar{n}_{xc}(\mathbf{r}, \mathbf{r} + \mathbf{u})}{u}, \tag{18}$$

where, in accordance with our notational conventions of section 1.3.

$$\bar{n}_{xc}(\mathbf{r}, \mathbf{r}') = \int_0^1 d\lambda \; n_{xc,\lambda}(\mathbf{r}, \mathbf{r}'). \tag{19}$$

Thus the real space decomposition of E_{xc} is given by

$$E_{xc} = \int d^3u \; E_{xc}(\mathbf{u}), \tag{20}$$

where

$$E_{xc}(\mathbf{u}) = \frac{N}{2} \langle \bar{n}_{xc}(\mathbf{u}) \rangle \frac{1}{u}, \tag{21}$$

and $\langle ... \rangle$ denotes a system-average, i.e.,

$$\langle \bar{n}_{xc}(\mathbf{u}) \rangle \equiv \frac{1}{N} \int d^3r \; n(\mathbf{r}) \; \bar{n}_{xc}(\mathbf{r}, \mathbf{r} + \mathbf{u}). \tag{22}$$

Clearly, from Eqs. (20-21), a good approximate functional need only get the angle-averaged $\langle \bar{n}_{xc}(\mathbf{u}) \rangle$ right in order to yield a good approximation for the exchange-correlation energy, and therefore for the total energy. This is why we study this exchange-correlation hole.

2.2. Exact conditions on the exchange-correlation hole

We may now list some of the simple physical conditions that the exact exchange-correlation hole satisfies. A common decomposition of the hole is into its separate exchange and correlation contributions. The exchange (or Fermi) hole is the hole due to the Pauli exclusion principle, and obeys the exact conditions:

$$n_x(\mathbf{r}\sigma, \mathbf{r}'\sigma') \le 0, \tag{23}$$

and

$$\int d^3r' \; n_x(\mathbf{r}\sigma, \mathbf{r}'\sigma') = -\delta_{\sigma,\sigma'} \tag{24}$$

The correlation hole obeys

$$\int d^3r' \; n_c(\mathbf{r}\sigma, \mathbf{r}'\sigma') = 0, \tag{25}$$

so that electrons of both spins are Coulombically repelled from the electron of spin σ at r, but accumulate in a bump at a finite distance away. The exchange conditions may be deduced from the fact that the non-interacting wavefunction is a Slater determinant, while the integral condition on the correlation hole comes from the normalization of the second order density matrix.

To understand these holes in more detail, we also consider their spin decomposition. Because the Hooke's atom is unpolarized, it has only two distinct spin combinations: parallel (↑↑) and antiparallel (↑↓). In Figures 3 and 4 we decompose the spin-averaged hole into these separate contributions. In fact the anti-parallel
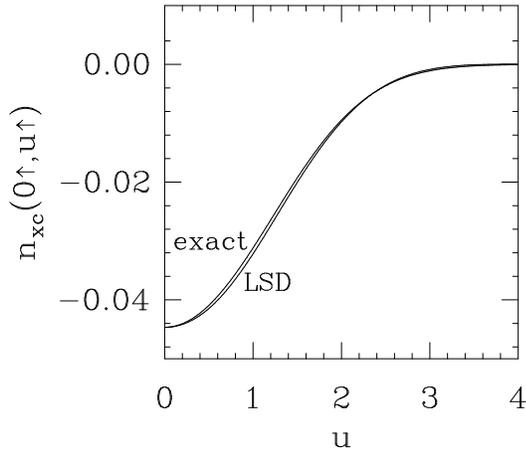
Figure 3. Parallel hole around a spin-up electron at the origin of Hooke's atom.
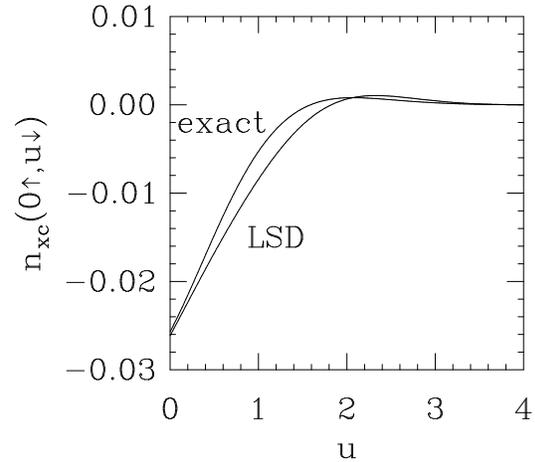
Figure 4. Anti-parallel hole around a spin-up electron at the origin of Hooke's atom.

hole is made up entirely of correlation. This is because, for exchange, a spin $\uparrow$ electron does not care about the distribution of spin $\downarrow$ electrons, i.e.,

$$g_x(\mathbf{r}, \uparrow; \mathbf{r}', \downarrow) = 1 \tag{26}$$

everywhere, so that

$$n_x(\mathbf{r}, \uparrow; \mathbf{r}', \downarrow) = 0. \tag{27}$$

Also, for a spin-unpolarized two-electron system like the Hooke's atom, the exact parallel hole is made up entirely of exchange. This can be seen most easily in the spin-decomposed second-order density matrix. Since the ground state wavefunction is a spin singlet, it contains no contribution in which both electrons have the same spin. Therefore

$$\rho_2(\mathbf{r} \uparrow, \mathbf{r}' \uparrow) = 0 \tag{28}$$

for both the exact and the exchange-only cases. Then, from Eqs. (11-12), we find

$$n_{xc}(\mathbf{r} \uparrow, \mathbf{r}' \uparrow) = n_x(\mathbf{r} \uparrow, \mathbf{r}' \uparrow) = -n_\uparrow(\mathbf{r}'). \tag{29}$$

Combining these two results tells us that Figure 3 is in fact the (spin-averaged) exchange hole, while Figure 4 is the (spin-averaged) correlation hole for this system, so that the integral relations Eqs. (24-25) apply. Note that the integrals include a factor of $4\pi u^2$, which weights the integrand, making the positive bump in Figure 4 contribute heavily. We also note that the exchange hole given by Eq. (29) obeys the general condition that the exchange hole be everywhere negative, Eq. (23).

Another more subtle condition is the electron-electron cusp condition. As two electrons approach each other, their Coulomb interaction dominates, and this leads to a cusp in the exchange-correlation hole at zero separation[15]. It is most simply expressed in terms of the pair distribution function. We define its spherically-averaged derivative at zero separation as

$$g'(\mathbf{r}, \mathbf{r}) = \left.\frac{\partial}{\partial u}\right|_{u=0} \int \frac{d\Omega_u}{4\pi} \, g(\mathbf{r}, \mathbf{r} + \mathbf{u}), \tag{30}$$

and the cusp condition is then[16]

$$g'(\mathbf{r}, \mathbf{r}) = g(\mathbf{r}, \mathbf{r}). \tag{31}$$

One can clearly see the cusp in the exchange-correlation hole of Figure 2. However, we may decompose this relation further. In fact, the cusp only occurs for antiparallel spins, as, by the exclusion principle, two parallel spins cannot have zero separation. Furthermore, the non-vanishing derivative is a pure correlation effect, as the exchange hole is the hole of a non-interacting system, which has no cusp. Thus we can write

$$g'_x(\mathbf{r}\sigma, \mathbf{r}\sigma') = 0, \tag{32}$$

and

$$g'_c(\mathbf{r}\sigma, \mathbf{r}\sigma') = (1 - \delta_{\sigma',\sigma}) \, g(\mathbf{r}\sigma, \mathbf{r}\sigma'). \tag{33}$$

This is borne out by the lack of any cusp in Figure 3. The electron-electron cusp condition is *not* obeyed by some popular approximations, e.g., the random phase approximation[17,**?**].

2.3. Scaling relations

Another type of exact condition comes from studying scaling relations of the exchange-correlation functional itself[19–25], a subject which has recently been reviewed by Levy[26]. We define a uniform scaling of the density by

$$n_\gamma(\mathbf{r}) = \gamma^3 n(\gamma \mathbf{r}), \tag{34}$$

and two non-uniform scalings by

$$n_\gamma^x(x, y, z) = \gamma n(\gamma x, y, z), \tag{35}$$

and

$$n_{\gamma\gamma}^{xy}(x, y, z) = \gamma^2 n(\gamma x, \gamma y, z), \tag{36}$$

so that the total number of electrons N remains fixed in all cases.

The fundamental scaling constraint on the total exchange-correlation energy under uniform scaling for all densities is[19]

$$E_{xc}[n_\gamma] > \gamma E_{xc}[n]; \qquad \gamma > 1. \tag{37}$$

In the low density limit, under both uniform and two-dimensional scaling, $E_{xc}/\gamma \to$ constant[21], i.e.

$$\lim_{\gamma \to 0} \frac{1}{\gamma} E_{xc}[n_\gamma] \equiv B[n] < E_{xc}[n], \tag{38}$$

and

$$\lim_{\gamma \to 0} \frac{1}{\gamma} E_{xc}[n_{\gamma\gamma}^{xy}] > -\infty. \tag{39}$$

In the high density limit, under one-dimensional scaling, we also find[21]

$$\lim_{\gamma \to \infty} E_{xc}[n_\gamma^x] > -\infty. \tag{40}$$

$E_{xc}[n]$ also obeys the Lieb-Oxford bound[27,28]:

$$E_{xc}[n] \geq -D \int d^3r \; n^{4/3}(\mathbf{r}), \tag{41}$$

where $1.44 \leq D \leq 1.68$.

In place of Eq. (37), the exchange energy obeys an equality under uniform scaling[19]

$$E_x[n_\gamma] = \gamma E_x[n], \tag{42}$$

while obeying Eqs. (39-40) under non-uniform scaling[21]. The correlation energy, on the other hand, obeys an inequality[19]

$$E_c[n_\gamma] > \gamma E_c[n]; \qquad \gamma > 1 \tag{43}$$

for all densities. For high densities, it tends to a constant under uniform scaling[20, 21], i.e.,

$$\lim_{\gamma \to \infty} E_c[n_\gamma] > -\infty, \tag{44}$$

but vanishes for one-dimensional scaling[22]:

$$\lim_{\gamma \to \infty} E_c[n_\gamma^x] = 0. \tag{45}$$

For low densities, $E_c[n]$ again tends to a constant under uniform scaling[21], i.e.,

$$\lim_{\gamma \to 0} \frac{1}{\gamma} E_c[n_\gamma] > -\infty, \tag{46}$$

but vanishes for two-dimensional scaling[22]:

$$\lim_{\gamma \to 0} \frac{1}{\gamma} E_c[n_{\gamma\gamma}^{xy}] = 0. \tag{47}$$

There also exist relations connecting the coupling-constant to uniform density scaling[21]:

$$E_{xc,\lambda}[n] = \lambda E_{xc,\lambda=1}[n_{1/\lambda}], \tag{48}$$

from which one may calculate the coupling-constant average using only the $\lambda = 1$ functional:

$$E_{xc}[n] = \int_0^1 d\lambda \; \lambda \; E_{xc,\lambda=1}[n_{1/\lambda}]. \tag{49}$$

One may also show that the exchange-correlation energy always decreases as a function of coupling-constant[19,21], i.e.,

$$\frac{\partial}{\partial\lambda} \; E_{xc,\lambda} \leq 0; \qquad\qquad \lambda \geq 0. \tag{50}$$

Note that $E_x[n]$ is independent of λ by definition, as

$$E_x[n] = E_{xc,\lambda=0}[n], \tag{51}$$

so the above relations, Eqs. (48-50), also apply to the correlation contribution alone. Lastly we mention that the coupling-constant dependence of the hole itself may also be extracted by scaling[21]:

$$n_{xc,\lambda}([n]; \mathbf{r}, \mathbf{r} + \mathbf{u}) = \lambda^3 n_{xc,\lambda=1}([n_{1/\lambda}]; \lambda\mathbf{r}, \lambda\mathbf{r} + \lambda\mathbf{u}). \tag{52}$$

2.4. Wavevector analysis

To conclude this section, we make a Fourier transform of the real space decomposition[12] of Eq. (20). If we write

$$n_{xc}(\mathbf{k}) = \int d^3u \; n_{xc}(\mathbf{u}) \exp(i\mathbf{k} \cdot \mathbf{u}), \tag{53}$$

then, from Eq. (21), we have

$$E_{xc} = \int \frac{d^3k}{(2\pi)^3} E_{xc}(\mathbf{k}), \tag{54}$$

where

$$E_{xc}(\mathbf{k}) = \frac{N}{2} \frac{4\pi}{k^2} \langle \bar{n}_{xc}(\mathbf{k}) \rangle. \tag{55}$$

where $\langle \bar{n}_{xc}(\mathbf{k}) \rangle$ is the Fourier transform of the real space system-averaged hole $\langle \bar{n}_{xc}(\mathbf{u}) \rangle$. The momentum space hole is simply related to the static structure factor of the system, as[12]

$$\bar{S}(\mathbf{k}) = 1 + \langle \bar{n}_{xc}(\mathbf{k}) \rangle, \tag{56}$$

which can be easily related to quantities more common in many-body diagrammatic treatments, such as the dynamic susceptibility[12].

These equations decompose E_{xc} into contributions from density fluctuations of various wavevectors k with wavelengths $2\pi/|\mathbf{k}|$. The relation between this Fourier decomposition and the real space analysis of the previous section is straightforward. The large distance behavior of the hole is determined by the small wavevector behavior of the structure factor. For the uniform gas, the structure factor is quadratic in k for small values of k, which means that the total hole decays as $1/u^5$. Note that both the exchange and correlation holes each separately decay only as $1/u^4$, but that these long tails cancel, yielding a more rapid decay of the total. This cancellation probably also occurs in finite inhomogeneous systems. Similarly, the short distance behavior in real space, especially the cusp of Eq. (31), determines the large wavevector behavior of $\bar{S}(\mathbf{k})$. This aspect is considered in more detail in constructing PW91, and in great detail in section 4.3.

3. LOCAL AND SEMILOCAL APPROXIMATIONS

In this section we define the local spin density (LSD) approximation, the work-horse of density functional theory. We then examine its extension to semilocal functionals, i.e., those which employ both the local density and its derivatives, also called generalized gradient approximations. We show how the PW91 functional obeys many exact conditions for the inhomogeneous system, as described in section 2, which earlier semilocal functionals do not.

All local and semilocal density functionals for the energy obey the important constraint of *size-consistency*, i.e., the energy of a system of well-separated fragments (e.g., separated atoms) is just the sum of the energies of the individual fragments, so that binding energy curves may be calculated. Such local and semilocal functionals typically make a self-interaction error, i.e., they are not exact for one-electron systems. However, energy functionals that avoid the self-interaction error through a dependence of the energy density upon the total number $N = \int d^3r \, n(\mathbf{r})$ of electrons are typically too nonlocal to achieve size-consistency.

3.1. Local spin density approximation

The LSD approximation to E_{xc} is defined as

$$E_{xc}^{LSD}[n_\uparrow, n_\downarrow] = \int d^3r \, n(\mathbf{r}) \, \epsilon_{xc}(n_\uparrow(\mathbf{r}), n_\downarrow(\mathbf{r})), \tag{57}$$

where $\epsilon_{xc}(n_\uparrow(\mathbf{r}), n_\downarrow(\mathbf{r}))$ is the exchange-correlation energy per particle of a uniform electron gas (jellium). This function is now well-known from Monte Carlo data[29,30], and has been accurately fitted to analytic forms[31,32]. The LSD approximation is thus a first-principles approximation, in the sense that no parameters are fitted empirically to better solutions or experimental values for other systems. It is exact for a uniform system, and a good approximation for slowly-varying systems. Furthermore, it has also been found to provide moderate accuracy for a large variety of systems in which the density varies rapidly, and which are therefore beyond the obvious range of validity. However, because the properties of many systems depend on relatively small energy differences, the LSD approximation can often produce the wrong ground state of a system. Another unfortunate feature, to be discussed below, is the lack (until recently) of any systematic approach to its improvement.

In terms of the exchange-correlation hole, we may write the LSD approximation as

$$n_{xc}^{LSD}(\mathbf{r}\sigma, \mathbf{r} + \mathbf{u}\sigma') = n_{xc}^{jell}(n_\uparrow(\mathbf{r}), n_\downarrow(\mathbf{r}); \sigma, \sigma', u), \tag{58}$$

where $n_{xc}^{jell}(n_\uparrow, n_\downarrow; \sigma, \sigma', u)$ is the spin-decomposed hole of the uniform electron gas (jellium) with spin densities $n_\uparrow$ and $n_\downarrow$ at separation u from the electron. Eq. (58) is expected to be most accurate for small u; see Figure 2 and subsection 4.3. If this approximation for the hole is inserted in Eqs. (20) and (21), one recovers Eq. (57) above.

We have made the LSD approximation to the quantities plotted in Figure 2-4, in which we see that LSD works very well. These plots were made using a

parameterization of the Monte Carlo data[33] whose spin analysis is currently being updated[34]. We point out that the LSD approximation works atypically well here, because the density has zero gradient at $r = 0$ in Hooke's atom, as shown in Figure 1. Furthermore, it has been shown (at least for the exchange piece) that the off-center (i.e. $r \neq 0$) hole can be very poorly approximated by the LSD expression above[35]. However, since the exchange-correlation energy depends only on the system-averaged, spherically-averaged, and spin-summed hole, the LSD can and does still work well for the complete exchange-correlation energy. We believe that much of the huge success of the LSD approximation may be attributed[36] to the fact that it obeys many of the exact relations known to be obeyed by non-uniform systems. It obeys these relations because the LSD approximation to the hole given in Eq. (58) above represents the hole of a physical system, the spin-polarized uniform gas, and therefore obeys all exact universal relations as they apply to that system. For example, the LSD approximation obeys all of the relations discussed in the previous section, except Eq. (44) and the non-uniform scaling relations, Eqs. (39), (40), (45), and (47). In some sense, given all those restrictions, it *cannot* do terribly badly.

A good example of how the LSD approximation does well because it uses a physical hole is given by the parallel correlation hole for the Hooke's atom. As discussed in section 2.2, this contribution to the hole is exactly zero, because the Hooke's atom is a spin-unpolarized two-electron system. However, the LSD approximation is a continuum approximation which has no explicit information about the number of electrons in the system, and therefore does not make this quantity vanish exactly everywhere. In Figure 5, we plot this hole and its LSD approximation on the same scale as the total parallel hole was plotted in Figure 3. At both zero and large separations, the LSD hole vanishes because $g_c(\uparrow, \uparrow, u) = 0$ as $u \to 0$ and as $u \to \infty$ for all densities in jellium. Furthermore, the integral of the hole in Figure 5 also vanishes. Thus its net contribution to the energy is very small compared with the rest of the hole, and the LSD approximation works well.

We note a very important point in density functional theory and the construction of approximate functionals. It is the hole itself which can be well-approximated by, e.g., a local approximation. This is because it is the hole which obeys the exact conditions we have been discussing. To illustrate this point, Figure 6 is a plot of the pair distribution function around the origin in Hooke's atom, both exactly and within the LSD approximation. We see that the two functions are quite different. In particular, the exact pair distribution function has not saturated even far from the center. The corresponding holes of Figure 2, on the other hand, are much more similar.

To be fair, there are several well-known exact conditions that the LSD approximation does *not* get right: it is not self-interaction free[37], $v_{xc,\sigma}^{LSD}(\mathbf{r})$ does not have the correct $-1/r$ behavior at large r for finite systems[38], it does not contain the integer discontinuity[39–41], etc. These shortcomings may be overcome by other improvements[42], but not by the gradient corrections discussed in this article.
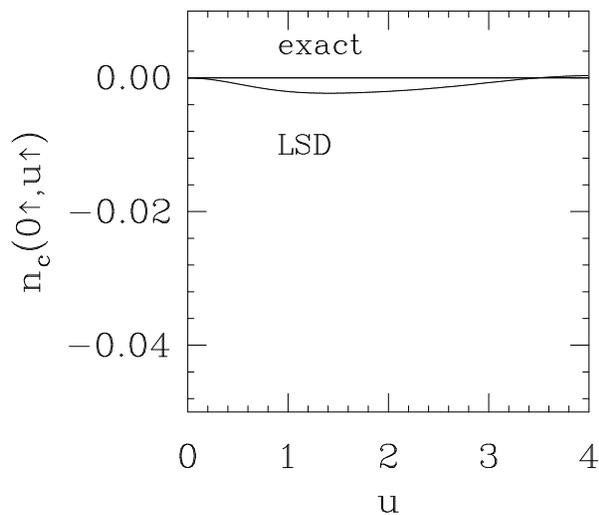
Figure 5. Parallel correlation hole around a spin-up electron at the origin of Hooke's atom.

3.2. Generalized gradient approximations

An obvious way to improve on the LSD approximation is to allow the exchange-correlation energy per particle to depend not only on the (spin) density at the point **r**, but also on the (spin) density gradients. This generalizes Eq. (57) to the form

$$E_{xc}^{GGA}[n_\uparrow, n_\downarrow] = \int d^3r \ f(n_\uparrow(\mathbf{r}), n_\downarrow(\mathbf{r}), \nabla n_\uparrow, \nabla n_\downarrow) \tag{59}$$

where the function f is chosen by some set of criteria. Such approximations are called generalized gradient approximations (GGA's), for reasons to be explained below, and a variety of different forms for the function f have been suggested and applied in the literature.

One way[43] to compare these GGA's (for spin-unpolarized systems) is to define the exchange-correlation enhancement factor $F_{xc}(r_s, s)$, by writing:

$$E_{xc}^{GGA}[n/2, n/2] = \int d^3r \ n(\mathbf{r}) \ \epsilon_x(n(\mathbf{r})) \ F_{xc}(r_s(\mathbf{r}), s(\mathbf{r})), \tag{60}$$

where $\epsilon_x(n) = -3k_F/4\pi$ is the exchange energy per particle for a uniform gas of density n,

$$s = |\nabla n|/(2k_F n) \tag{61}$$

is a dimensionless measure of the gradient, with the local Fermi wavevector defined as

$$k_F = (3\pi^2 n)^{1/3}, \tag{62}$$
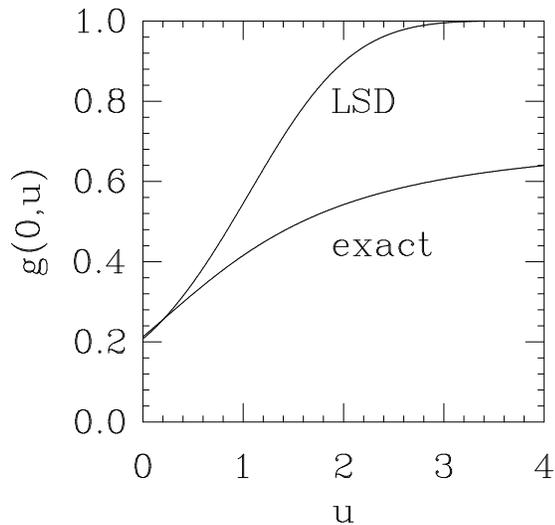
Figure 6. Pair distribution function around an electron at the origin of Hooke's atom.

and r_s is the local Wigner-Seitz radius,

$$r_s = (4\pi n/3)^{-1/3}. \tag{63}$$

Thus $F_{xc}(r_s, s)$ is a measure of the enhancement in the energy per particle over local exchange. In the rest of this subsection, we plot curves of $F_{xc}(r_s, s)$ for different approximations for several values of r_s. The energies of real systems can contain significant contributions from s up to about 3, and r_s up to about 18. Valence electrons in solid metals have $s \lesssim 2$ and $1 \lesssim r_s \lesssim 6$. In the core of an atom, $s \lesssim 1$ and $r_s \lesssim 1$. In the limit $r \to \infty$ for a finite system, r_s and s grow exponentially.

Figure 7 is a plot of F_{xc} in the LSD approximation. The curves are horizontal lines in this case, as the LSD approximation is independent of the local gradient. However, only in the high density limit, $r_s = 0$, is $F_{xc} = 1$, because this is where exchange dominates. The increase in F_{xc} beyond 1 for finite values of r_s represents the correlation contribution to the exchange-correlation energy. The LSD approximation obeys all the conditions of section 2 except Eqs. (39), (40), (44), (45), and (47), because it approximates the hole by a hole taken from another physical system.

The gradient expansion approximation (GEA) was suggested by Kohn and Sham[6], and is found by considering the LSD approximation as the first term in a Taylor series for $E_{xc}[n_\uparrow, n_\downarrow]$ about the uniform density, and adding in the next corrections. Such an expansion can be rigorously performed. The first corrections to the LSD approximation are in principle straightforward to calculate, and the addition of these leading corrections to the exchange-correlation energy functional produces
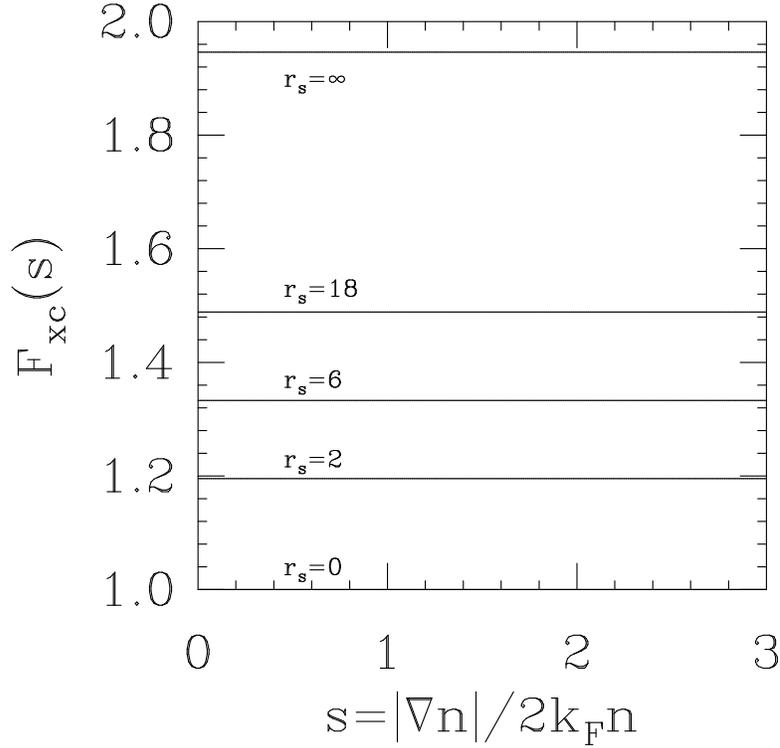
Figure 7. $F_{xc}(s)$ for LSD.

the GEA:

$$E_{xc}^{GEA}[n_\uparrow, n_\downarrow] = \int d^3r \left[n(\mathbf{r}) \, \epsilon_{xc}(n_\uparrow(\mathbf{r}), n_\downarrow(\mathbf{r})) + \sum_{\sigma,\sigma'} C_{\sigma,\sigma'}(n_\uparrow(\mathbf{r}), n_\downarrow(\mathbf{r})) \frac{\nabla n_\sigma}{n_\sigma^{2/3}} \cdot \frac{\nabla n_\sigma'}{n_{\sigma'}^{2/3}} \right] \qquad (64)$$

where the coefficients $C_{\sigma,\sigma'}(n_\uparrow, n_\downarrow)$, which are slowly-varying functions of the density, have been calculated by Rasolt and collaborators[44,45]. Since the GEA is designed to include only the second-order gradient contributions, all the curves of $F_{xc}^{GEA}(r_s, s)$ are parabolic in s, as shown in Figure 8.

Unfortunately, while the gradient correction is an improvement over LSD for slowly-varying systems, it typically worsens results on real electronic systems, which contain regions of rapidly varying density. If we compare Figure 8 with Figure 14 (PW91), which we treat as the "best" presently available functional by the criteria discussed in this article, we see that the small s behavior is only valid for very small values of s, and its extrapolation to realistic values of s leads to highly incorrect results. The GEA is the only approximation discussed here whose F_{xc} bends *downwards* for all s, and so fails to reduce to F_x when $r_s \to 0$. We claim that a principal reason for this failure is the fact that the exchange-correlation
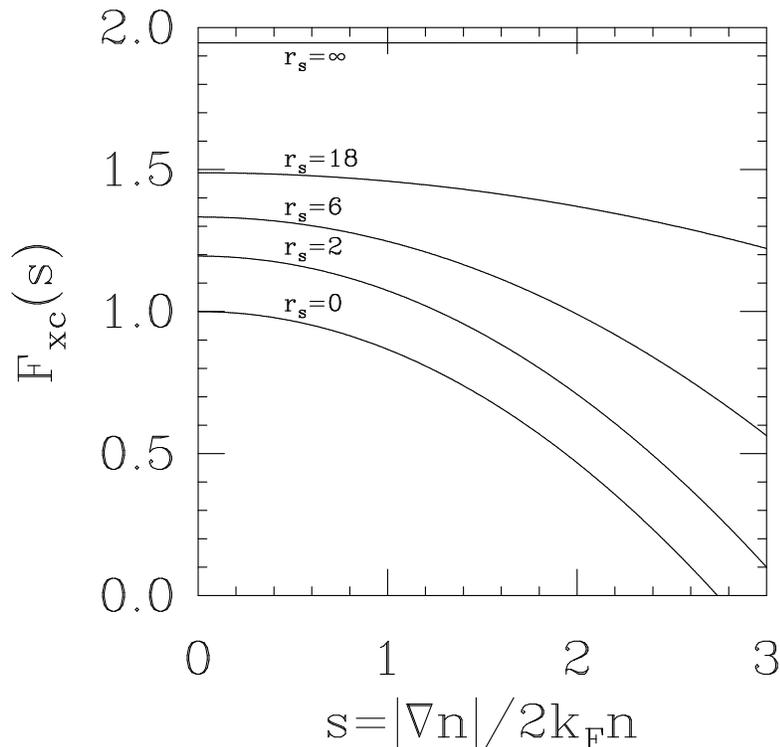
Figure 8. $F_{xc}(s)$ for GEA.

hole associated with the GEA above is *not* the hole of *any* physical system, and so it disobeys many of the exact conditions discussed in the previous section. In particular, it violates[46,47] even the sum rules Eqs. (24-25).

One way around this problem is to make a true GGA, where the function f is often chosen so as to reproduce the GEA form for slowly-varying densities, but contains all powers of ∇n_σ, and the higher powers may be chosen by some criteria to produce (one hopes) an improvement on the LSD approximation.

Early work going beyond the GEA was initiated by Ma and Brueckner[48], and Langreth and co-workers[49,50]. The most popular functional to come out of this work is the Langreth-Mehl (LM)[49], whose F_{xc} is plotted in Figure 9. This functional was constructed from a wavevector analysis[46] of $E_{xc}(\mathbf{k})$ within the random phase approximation (RPA). Essentially, the full GEA for exchange was retained, while the spurious small k contribution to the gradient term in the correlation energy was replaced by zero for $k < f|\nabla n|/n$, where the cutoff parameter $f = 0.15$ was adjusted to provide an overall fit to the correlation energies of atoms and metal surfaces; $f \approx 1/6$ had been expected on theoretical grounds. By studying Figure 9,
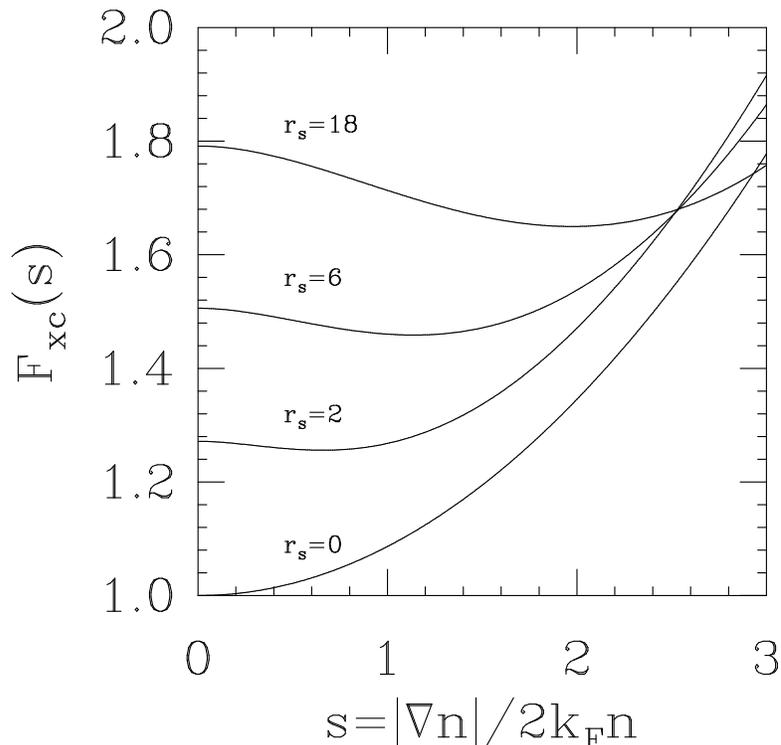
Figure 9. $F_{xc}(s)$ for LM.

we immediately see that LM cures the poor behavior of the GEA, by not extrapolating the downward trend near $s = 0$ to all s. Also, it looks somewhat like the PW91 F_{xc} of Figure 14, so it can be expected to improve LSD in the right directions. However, we also point out some of its more major shortcomings. Clearly, for $s = 0$, the curves do not agree with the LSD values of Figure 7, so the uniform gas limit is not correct. Also, notice that some of the curves cross each other. This violates the fundamental scaling constraint on E_{xc} of Eq. (37). For a uniform scaling of the density, s at the scaled point does not change, but n does. Thus, Eq. (37) implies

$$F_{xc}(r'_s, s) > F_{xc}(r_s, s); \qquad\qquad r'_s > r_s, \tag{65}$$

which LM clearly violates. Finally, we note that the $r_s = 0$ curve grows parabolically for all s. This is also incorrect, as the Lieb-Oxford bound implies[24,28] that F_{xc} has a finite $s \to \infty$ limit. This bound will be satisfied for all densities if

$$F_{xc}(r_s, s) \leq 2.27. \tag{66}$$

We turn next to Perdew-Wang 86 (PW86)[51,52], plotted in Figure 10. The PW86
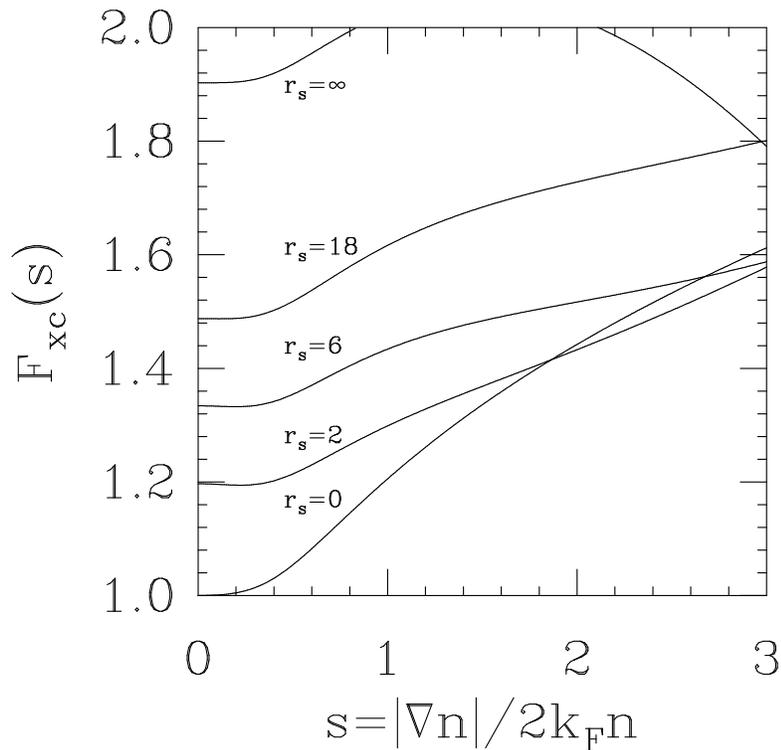
Figure 10. $F_{xc}(s)$ for PW86.

exchange energy functional[52] starts from the second-order gradient expansion for the exchange hole, then eliminates spurious large u contributions via sharp real-space cutoffs designed to restore the exact conditions, Eqs. (23-24). The result is a numerically defined GGA which is then fitted to an analytic form; this real-space cutoff procedure is free from semi-empirical parameters. In contrast, the PW86 correlation energy is constructed via a wavevector-space cutoff procedure similar to that of Langreth and Mehl[49], although PW86 includes beyond-RPA inputs for the uniform and slowly-varying electron gases. Since Eq. (25) is satisfied for any choice of the cutoff wavevector $f|\nabla n|/n$ where $f > 0$, the parameter f is found by fitting the correlation energy of the neon atom.

We see that PW86 includes both the correct uniform gas limit and the GEA by having the right s^2 dependence. It still has curve-crossing problems, but not as severe as LM. It violates the Lieb-Oxford bound, Eq. (66), and the exact condition

$$F_c(r_s, s) > 0. \tag{67}$$

which follows from Eq. (65). We can extract $F_c(r_s, s)$ from these figures for any non-zero value of r_s, since $r_s = 0$ gives the exchange contribution, i.e.,

$$F_c(r_s, s) = F_{xc}(r_s, s) - F_{xc}(r_s = 0, s), \tag{68}$$

so we see that Eq. (67) is violated by PW86.

A later modification of PW86 was based on the introduction of the Becke functional for exchange[53]. This functional was designed to recover the correct asymptotic behavior of the exchange energy density as $r \to \infty$ in finite systems. It contained a single adjustable parameter, which was fitted to achieve minimum error for a large number of atoms. This exchange functional was then combined with the PW86 correlation functional to form Becke-Perdew (BP)[53,51], a popular functional in the chemistry literature, whose F_{xc} is shown in Figure 11. We can see
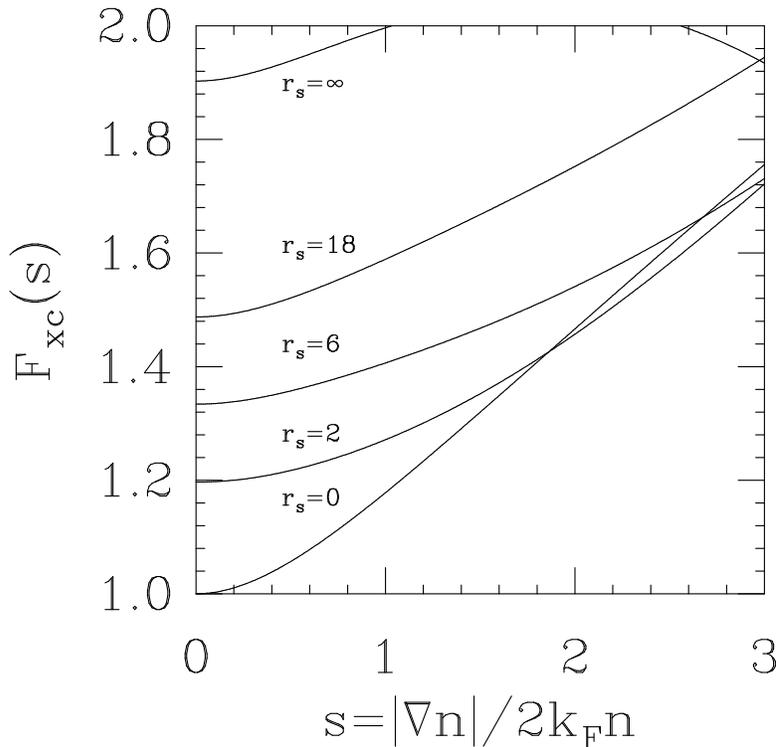

Figure 11. $F_{xc}(s)$ for BP.

that, both qualitatively and quantitatively, BP and PW86 are very similar. (One difference is that BP does not reduce to the correct GEA for small values of s.)

The real-space cutoff of the gradient expansion for the exchange hole thus justifies Becke's exchange functional.

A more recent correlation functional is that of Lee, Yang, and Parr[54], which is often used in conjunction with Becke exchange to form BLYP. The enhancement factor for BLYP is plotted in Figure 12. The LYP functional starts from the Colle-
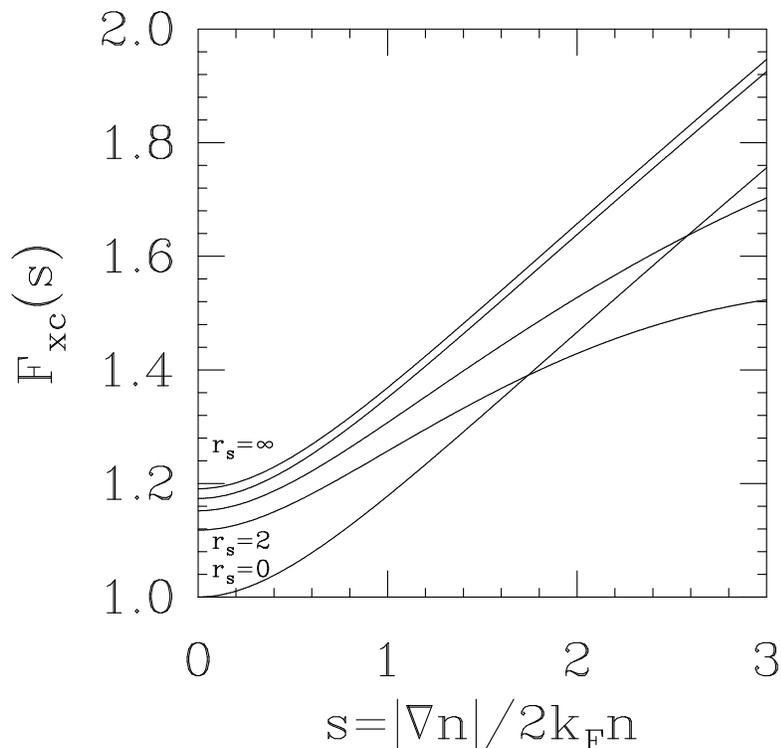
Figure 12. $F_{xc}(s)$ for BLYP; the two unlabeled curves are for $r_s = 6$ (lower) and $r_s = 18$ (higher).

Salvetti formula for the correlation energy in terms of the electron density and the non-interacting kinetic energy density, then replaces the latter by its second-order density-gradient expansion. (The Colle-Salvetti formula itself is derived from a number of theoretical approximations, and is fitted to the correlation energy of the helium atom.) The result is then cast into the GGA form of Eq. (59) via integration by parts[55].

Clearly, BLYP is inaccurate in the uniform limit ($s = 0$), and violates Eq. (37) via curve-crossing. LYP also violates[56] Eqs. (43), (45), (47), and (66), but does satisfy the high density uniform scaling relation, Eq. (44). A way of modifying PW91 to

obey this relation is discussed in section 4.1.

Next we examine another correlation functional, called Wilson-Levy (WL)[57]. Figure 13 is a plot of F_{xc} for BWL, which uses Becke exchange and WL correlation. The WL correlation functional was designed to obey a few, but not all, of the scaling
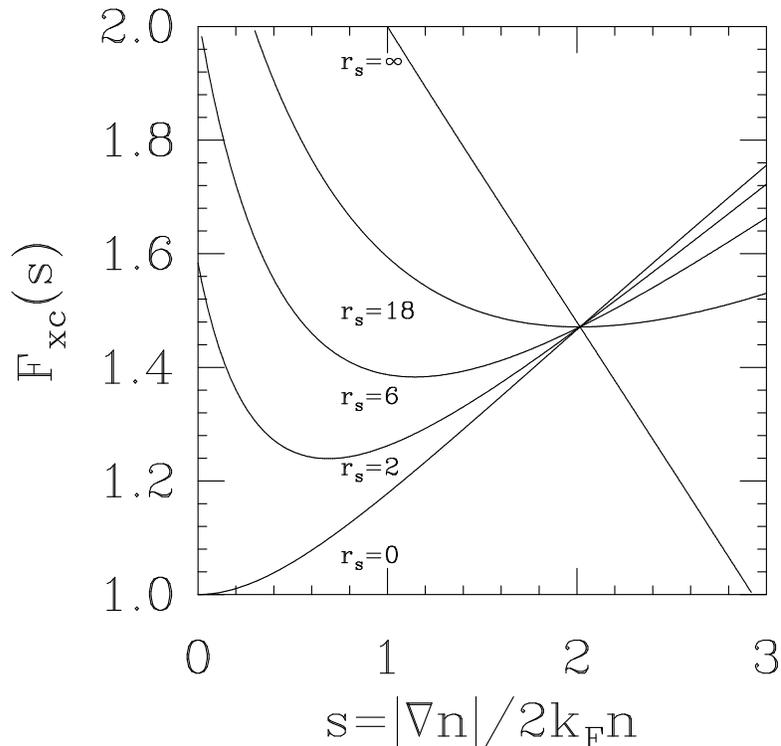
Figure 13. $F_{xc}(s)$ for BWL.

relations that were known at the time. Starting from a Wigner-like form with gradient corrections, the coefficients in this functional were adjusted to minimize $\left[\partial E_c[n_\lambda]/\partial\lambda\right]^2$ for eight closed-shell atoms, while fitting the correlation energy of the He atom. We see that BWL is inaccurate in the uniform ($s = 0$) and slowly-varying ($s \ll 1$) limits, and violates Eq. (37). WL also violates the recently-discovered non-uniform scaling constraints, Eqs. (45) and (47).

Lastly, we discuss the Perdew-Wang 91 (PW91)[58,28,43,59] functional. Like LSD and GEA, and unlike all the other GGA's discussed here, PW91 is *ab initio*, in the sense that it was constructed using only uniform electron gas data (both ground-state and linear response), along with the exact conditions discussed in section 2. PW91 was constructed from a real-space cutoff procedure for the spurious large

u part of the exchange-correlation hole produced by GEA. The sharp cutoffs were chosen to restore Eqs. (23)-(25). No semi-empirical parameters were fitted to atomic systems. Its F_{xc} is plotted in Figure 14. It was designed to obey many of the exact
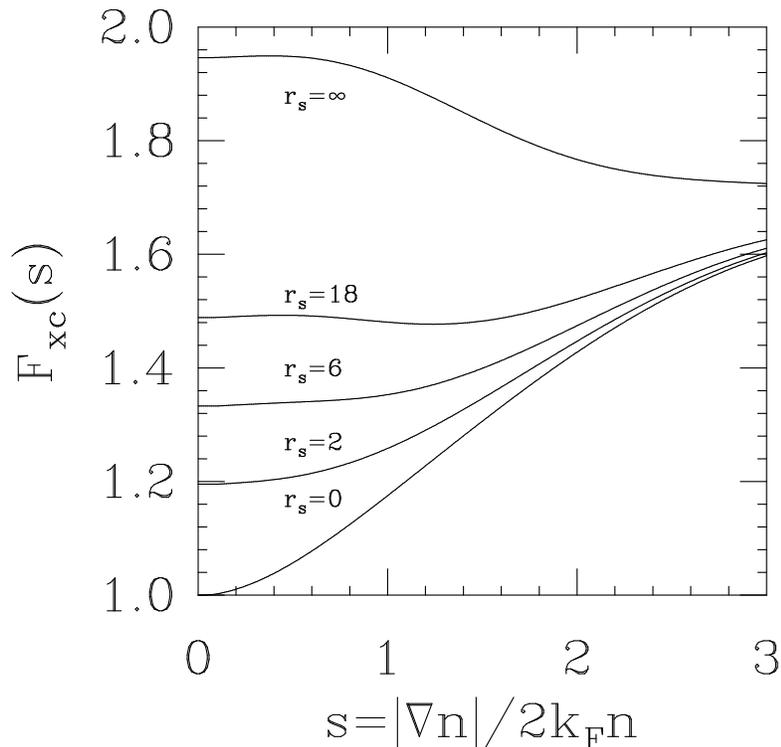
Figure 14. $F_{xc}(s)$ for PW91.

scaling relations which were known at the time of construction, and turns out to obey exactly or approximately many that have been found since.

Note that PW91 becomes more local as the density is reduced. The explanation is that, as n decreases from ∞ to 0, the hole density at the origin drops from $-n/2$ to $-n$, and, because it integrates to exactly -1, it becomes more localized, on the scale of the Fermi wavelength.

Concerning conditions PW91 gets right, we first note its recovery of the uniform and almost-uniform gas limits. We also see that curves do not cross in Figure 14, so PW91 obeys the fundamental uniform scaling relation, Eq. (37). Also F_c is positive for realistic densities (but see Ref. [56] for the extreme high density limit), and $F_{xc} \leq 1.93$, so the Lieb-Oxford bound, Eq. (66) is obeyed. PW91 also obeys the non-uniform scaling relations, Eqs. (39), (40), (45) and (47), whereas all the others

mentioned here do not.

The GGA form of Eq. (59) or Eq. (60) is of doubtful utility for $s \gg 1$, and the real-space cutoff of the GEA provides little guidance in this regime. Indeed, various exact conditions can lead to contradictory $s \to \infty$ limits for $F_{xc}(r_s, s)$. Because the PW91 correlation energy functional automatically satisfies the non-uniform scaling relations Eqs. (45) and (47), the PW91 exchange energy functional is chosen to satisfy to satisfy Eqs. (39) and (40), i.e.,

$$\lim_{s \to \infty} s^{1/2} F_{xc}(r_s, s) < \infty. \tag{69}$$

and the Lieb-Oxford bound, Eq. (41), as well. Although it is not apparent in Figure 14, $F_{xc}(r_s, s)$ decreases to zero as $s \to \infty$. However, Engel et al.[60] have shown that, to achieve the expected $-1/r$ behavior of $v_{xc}(r \to \infty)$ for finite systems, $F_{xc}(r_s, s)$ must *increase* as s when $s \to \infty$. Becke's exchange functional[53], which increases as $s/\ln s$ when $s \to \infty$, does not achieve this behavior. Lacks and Gordon[61] found that still a different large s behavior ($\approx s^{2/5}$, as in PW86) is needed to model the interaction between rare-gas atoms at large separation.

Amongst the functionals discussed in this subsection, it is unclear which exchange energy functional is to be preferred: PW86 (which emerges directly from a real-space cutoff of the gradient expansion of the exchange hole), Becke (which best fits the exchange energies and exchange-energy densities of atoms), or PW91 (which has the correct gradient expansion, satisfies the non-uniform scaling limits, and respects the Lieb-Oxford bound, by construction). In practice, there is usually not much difference between these three, and all are consistent with the real-space cutoff idea. On the other hand, the PW91 correlation energy functional seems the best choice in its class: it emerges directly from a real-space cutoff of the gradient expansion for the correlation hole, and automatically satisfies all the exact conditions of section 2 except the high density limit of uniform scaling, which it almost obeys (see subsection 4.1).

4. RECENT PROGRESS IN UNDERSTANDING EXACT CONDITIONS

We have seen in the previous two sections how knowledge of those exact conditions the LSD approximation obeys was vital to the construction and testing of PW91, and how its success relative to earlier GGA's can be attributed to these conditions. We believe that the construction of better functionals is intimately linked to improvements in our understanding of these conditions. In this section we present some results of more recent investigations, which were undertaken since the construction of PW91.

4.1. A slight formal improvement on PW91

In section 3.2, we noted that BLYP satisfies one condition that even PW91 gets wrong, namely that in the high density uniform scaling limit, E_c tends to a constant, Eq. (44). Recently, Levy and Perdew[24] have suggested a small change to the original PW91 which allows this condition to be satisfied, while retaining all the other good features of PW91. We denote this slightly modified version of PW91 as Perdew-Wang-Levy, or PWL[26]. However, this change is so small that F_{xc} for

PWL is indistinguishable from that of PW91 for the curves plotted in Figure 14. To illustrate the scale of the difference, in Figures 15-16 we plot several high density curves of the correlation contribution F_c for both these functionals. Note
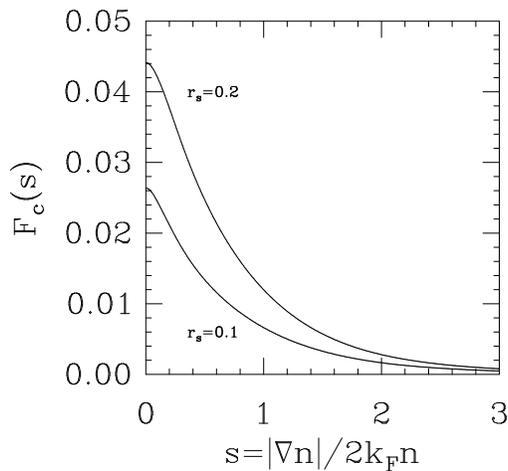
Figure 15. High density F_c for PW91.   Figure 16. High density F_c for PWL.
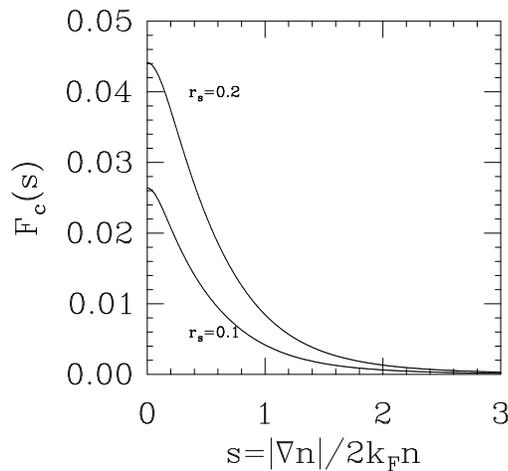
the densities, the scale of the y-axes, and the similarity of the curves.

This change is small, except for high densities and substantial gradients. Therefore we do not recommend the use of PWL in place of PW91. However, it should be noted that in some cases, this change can be important, e.g., there is a 10% change in the correlation energy of Ne.

4.2. Convexity constraint: A severe test at low density

Levy and Perdew[24] recently derived a very severe low density convexity constraint on E_{xc}. Define the convex functional $A[n]$ by

$$A[n] = \lim_{\gamma \to 0} \frac{1}{\gamma} E_{xc}[n_\gamma] + \frac{1}{2} \int d^3r \int d^3r' \frac{n(\mathbf{r})\, n(\mathbf{r}')}{|\mathbf{r} - \mathbf{r}'|}. \tag{70}$$

The convex condition is

$$A[d_1 n_1 + d_2 n_2] \leq d_1 A[n_1] + d_2 A[n_2], \tag{71}$$

where $n_i \geq 0$, $\int d^3r n_i(\mathbf{r}) = N$, $d_i \geq 0$, and $d_1 + d_2 = 1$. Equivalently, when the second functional derivative can be taken, we have

$$\left. \frac{\partial^2 A[n + \epsilon \Delta n]}{\partial \epsilon^2} \right|_{\epsilon=0} \geq 0, \tag{72}$$

or

$$\int d^3r \int d^3r' \left(\frac{\delta^2 A[n]}{\delta n(\mathbf{r}) \, \delta n(\mathbf{r}')} \right) \Delta n(\mathbf{r}) \Delta n(\mathbf{r}') \geq 0, \tag{73}$$

for arbitrary $\Delta n(\mathbf{r})$ such that $\int d^3r \, \Delta n(\mathbf{r}) = 0$ and $\Delta n(\mathbf{r}) \geq 0$ for all points where $n(\mathbf{r}) = 0$.

The condition that $A[n]$ is convex, i.e., Eqs. (71), (72), or (73), is a very difficult constraint to satisfy. For instance, with the LSD approximation for $A[n]$, one obtains

$$\left. \frac{\partial^2 A^{LSD}[n + \epsilon \Delta n]}{\partial \epsilon^2} \right|_{\epsilon=0} = -\frac{4}{9}|c| \int d^3r \, n^{-2/3}(\mathbf{r}) \Delta n(\mathbf{r})^2 + \frac{1}{2} \int d^3r \int d^3r' \frac{\Delta n(\mathbf{r}) \, \Delta n(\mathbf{r}')}{|\mathbf{r} - \mathbf{r}'|}, \tag{74}$$

where c is a constant. Eq. (74) clearly violates constraint Eq. (72). Observe, for example, that the first term becomes $-\infty$ with any $\Delta n(\mathbf{r})^2$ which vanishes more slowly than $n^{2/3}(\mathbf{r})$ as $|\mathbf{r}| \to \infty$.

From the above analysis, it is expected that virtually all present approximations to E_{xc}, including all the GGA's discussed in this paper, violate the convexity condition, because virtually all approximations contain a $-\int d^3r \, n^{4/3}(\mathbf{r})$ component, and it is, unfortunately, difficult to overcome the concavity of this component as $\gamma \to 0$. Along these lines, it has been shown[24] that the LSD approximation and PW91 do not satisfy Eq. (71) for the one-electron densities $n_1(\mathbf{r}) = \pi^{-1} \, e^{-2r}$ and $n_2(\mathbf{r}) = (4\pi)^{-1} \, (1 + 2r) \, e^{-2r}$. All this means that the satisfaction of the low density convexity requirement represents a tough challenge for the future.

4.3. Is the LSD approximation exact "locally"?

The LSD approximation treats the exchange-correlation hole around a point $\mathbf{r}$, $n_{xc}(\mathbf{r}, \mathbf{r}+\mathbf{u})$, as if the surrounding electronic distribution were uniform, as expressed by Eq. (58). The gradient expansion adds corrections to this based on the gradient of the density at the point $\mathbf{r}$. Clearly such a procedure will be worst for large values of u, where the density can be very different from that at $\mathbf{r}$, and work best for small values of u. Close inspection of Figure 2 shows that indeed the LSD hole is either identical or very close to the exact hole as $u \to 0$. In this section, we explore just how good the LSD approximation is as $u \to 0$, i.e., "locally", in the neighborhood of the electron at $u = 0$.

Almost twenty years ago, this question was addressed from a slightly different perspective in a series of papers by Langreth and Perdew[62,12,63,46,64]. In these papers, Langreth and Perdew studied the Fourier decomposition of the exchange-correlation hole, as introduced in section 2.4. They gave two arguments in favor of what we call the short wavelength hypothesis, namely that the LSD approximation is exact for short wavelengths (i.e., large k) for all inhomogeneous systems. This idea has considerable intuitive appeal, as the LSD is supposed to account for local behavior correctly. In fact, this hypothesis has since passed into the literature as one of the reasons for the success of the LSD approximation[13,14], and the LSD behavior for large wavevectors (or small interelectronic distances) has been incorporated in the LM, PW86, and PW91 GGA's discussed above.

The first argument was based on the result of a second order (in e^2) calculation of $E_{xc}(\mathbf{k})$ for a spin-unpolarized surface. They found that for large k, $E_{xc}^{(2)}(\mathbf{k})$ is

explicitly a local functional of the density, where the superscript indicates the number of powers of e^2 retained. Then, since the Coulomb interaction is $4\pi e^2/k^2$ in momentum space, they argued that all higher powers would be vanishingly small for large k, and so the short wavelength hypothesis would be valid in general.

The second argument came from the density functional version of the random phase approximation[63,46]. Within that scheme, they found that for any spin-unpolarized system, the leading gradient corrections to $E_{xc}^{LSD}(\mathbf{k})$ became vanishingly small as $k \to \infty$.

We have recently studied this short wavelength hypothesis in considerable detail[**?**]. We showed that the short wavelength hypothesis is correct for several limiting regimes and for certain approximate treatments of the inhomogeneous gas. However, we also found that the short wavelength hypothesis is *not* exact in general.

The key step in our proof is an exact analysis of the large wavevector behavior of an inhomogeneous system. To get a quantity which depends only on k, we define the angle-averaged wavevector decomposition

$$E_{xc}(k) = \int \frac{d\Omega_k}{4\pi} E_{xc}(\mathbf{k}). \tag{75}$$

A simple Fourier analysis of the asymptotic expansion for large k then yields[65]

$$E_{xc}(k) \approx \frac{\bar{C}}{k^6} + O(\frac{1}{k^8}), \tag{76}$$

where

$$C_\lambda = 16\pi^2 e^2 \int d^3r \; n^2(\mathbf{r}) \; g'_\lambda(\mathbf{r}, \mathbf{r}). \tag{77}$$

Here we have presented restored powers of e^2 explicitly, as we will later do perturbation theory in powers of the Coulomb repulsion. The bar over C denotes an average over the coupling constant λ, as discussed in section 1.3.

Physically, C, which controls the large wavevector decay of $E_{xc}(k)$, depends on the behavior of the system at small interelectronic separations. In fact, C is proportional to the system-average of the cusp in the exchange-correlation hole at zero separation. If $g_\lambda(\mathbf{r}, \mathbf{r}')$ were a smooth function of $\mathbf{r}' - \mathbf{r}$, then $g'_\lambda(\mathbf{r}, \mathbf{r}) = 0$, and C would vanish, as it does at the exchange-only level (i.e., to first order in e^2). However, as we saw in section 2.2, the singular nature of the Coulomb interaction between the electrons leads to the electron-coalescence cusp condition, Eq. (31). For the present purposes, we wish to keep track explicitly of powers of the coupling constant, so we rewrite Eq. (31) as

$$g_\lambda(\mathbf{r}, \mathbf{r}) = \lambda e^2 \; g'_\lambda(\mathbf{r}, \mathbf{r}). \tag{78}$$

Using this in Eq. (77) yields

$$C_\lambda = 16\pi^2 \lambda e^4 \int d^3r \; n^2(\mathbf{r}) \; g_\lambda(\mathbf{r}, \mathbf{r}). \tag{79}$$

These results are exact and apply to any inhomogeneous system. They reveal an intimate connection between the wavevector analysis[49,12,46] of E_{xc} for $k \to \infty$

and the real-space analysis of Section 2 at $\mathbf{u} = 0$. In fact, the real-space exchange-correlation hole at zero separation is simply related to $\bar{C}$ by

$$\langle n_{xc,\lambda}(\mathbf{u} = \mathbf{0})\rangle = \frac{C_\lambda}{16\pi^2\lambda e^4} - \int d^3r \; n^2(\mathbf{r}). \tag{80}$$

In terms of Eq. (76), the short wavelength hypothesis is that $\bar{C}_{LSD}$, the value of $\bar{C}$ found in an LSD calculation, is equal to the exact value of $\bar{C}$. $\bar{C}_{LSD}$ is found from Eq. (79), averaged over λ, and replacing $g_\lambda(\mathbf{r}, \mathbf{r})$ by its value for a uniform electron gas with spin densities equal to those at $\mathbf{r}$. Clearly, from Eq. (80), if the short wavelength hypothesis is exact (for each value of λ), then $\langle \bar{n}_{xc}(\mathbf{u} = \mathbf{0})\rangle$ is given exactly by the LSD approximation. This is what we mean by asking if the LSD approximation is exact "locally," i.e., does it produce the exact hole at zero separation?

Although $\bar{C}$ does indeed depend only on the pair distribution function at zero separation, this quantity is nevertheless a non-local functional of the density, invalidating the short wavelength hypothesis. (We show this later with an explicit example.) On the other hand, for high densities, the Hartree-Fock approximation is valid, and $g_\lambda(\mathbf{r}, \mathbf{r}) = (1 - \zeta^2(\mathbf{r}))/2$, where $\zeta(\mathbf{r}) = (n_\uparrow(\mathbf{r}) - n_\downarrow(\mathbf{r}))/n(\mathbf{r})$ is the relative spin-polarization at $\mathbf{r}$, so that

$$\bar{C}^{(2)} = 4\pi^2 e^4 \int d^3r \; n^2(\mathbf{r}) \left(1 - \zeta^2(\mathbf{r})\right), \tag{81}$$

where the superscript indicates the number of powers of e^2 retained, as for high densities and large wavevectors the Coulomb potential may be treated perturbatively. (Note that the cusp condition of Eq. (78) has bought us an extra factor of e^2 in Eq. (81).) Thus $\bar{C}^{(2)}$ is explicitly a local functional of the density and spin-polarization, and the short wavelength hypothesis is true in the high-density limit. In the early work, this result was found by an explicit calculation of $E_{xc}(k)$ for large k for a spin-unpolarized surface (appendix D of Ref. [12]). Eq. (81) represents a considerable generalization of that second-order perturbation theory result, to all inhomogeneous systems for any spin-polarization.

We note that the short wavelength hypothesis is also absolutely (if not relatively) exact in two other limits. For either fully spin-polarized systems, or in the low density limit, $g_\lambda(\mathbf{r}, \mathbf{r}) = 0$, both exactly and in the LSD.

We next examine the short wavelength behavior of $E_{xc}(k)$ within the RPA. Throughout this paper, the RPA for the inhomogeneous case is the density-functional version of the RPA[63], in which the non-interacting susceptibility, from which the interacting susceptibility is calculated, is taken to be the λ-independent, single-particle response of the electrons in the Kohn-Sham potential. This approximation is very poor at small separations, and does not obey the exact cusp condition Eq. (78). In fact, within the RPA, for both the homogeneous[17] and inhomogeneous cases[65],

$$g'_\lambda(\mathbf{r}, \mathbf{r}) = \lambda e^2. \qquad \text{(RPA)} \tag{82}$$

Inserting this cusp in Eq. (77) produces the RPA value of $\bar{C}$,

$$\bar{C}_{RPA} = 8\pi^2 e^4 \int d^3r \; n^2(\mathbf{r}). \tag{83}$$

Note that this result gives $\bar{C}_{RPA}$ for *all* densities, not just in the high-density limit.

Thus indeed the short wavelength hypothesis is exact within RPA, but is entirely an artifact of the error RPA makes at small separations. In the earlier work of Langreth and Perdew[63,46], the leading gradient corrections to LSD were calculated explicitly, and found to vanish for large k. The present result confirms that aspect of that calculation, and shows that indeed *all* gradient corrections vanish for large k within RPA, but that the RPA is a terrible approximation for these quantities anyway.

Clearly, by adding second-order exchange to the RPA, we find $\bar{C}_{RPA2X} = \bar{C}^{(2)}$, as given by Eq. (81), for which the short wavelength hypothesis *is* exact. If this produced a good approximation to $\bar{C}$ for all systems, then we would have a strong justification for the approximate validity of the short wavelength hypothesis. However, we can see that this is not the case, even in the spin-unpolarized uniform electron gas. In that case, from performing the coupling-constant integration on Eq. (79), we find $\bar{C} = 16\pi^2 e^4 n N \bar{\bar{g}}(0)$, where

$$\bar{\bar{g}}(0) = \int_0^1 d\lambda \, \lambda \, g_\lambda(0). \tag{84}$$

Figure 17 is a plot of $\bar{\bar{g}}(0)$ as a function of r_s for the uniform gas. It was made using Yasuhara's ladder-diagram expression[66] for $g(0)$ as a function of r_s, as parameterized by Perdew and Wang[33], and confirmed by Quantum Monte Carlo calculations[67,29,30]. Only at high densities does the RPA2X result agree well with the exact value.
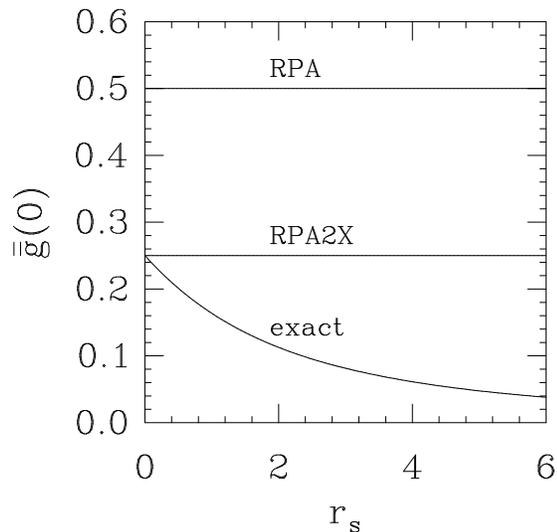

Figure 17. $\bar{\bar{g}}(0)$ for unpolarized uniform electron gas

Although we have pointed out the limitations of earlier arguments in favor of the short wavelength hypothesis, we have not yet explicitly shown how it fails. This is most easily done by considering corrections to the high density limit. If we write $\bar{C} = \bar{C}^{(2)} + \bar{C}^{(3)} + ...$, we find, for the spin-unpolarized case,

$$\bar{C}^{(3)} = -\alpha \frac{8\pi^2 e^6}{3} \int d^3r \; n^2(\mathbf{r}) \; r_s(\mathbf{r}), \tag{85}$$

where $r_s(\mathbf{r}) = (4\pi n(\mathbf{r})/3)^{-1/3}$, and α is a system-dependent dimensionless constant. (If the short wavelength hypothesis were correct, α would be universal!). For the uniform electron gas, Eq. (85) implies

$$g(0) = 1/2 \; (1 - \alpha \; r_s + ...), \tag{86}$$

and the value of α has been calculated as[68,69]

$$\alpha = (4/9\pi)^{1/3} \; 2 \; (\pi^2 + 6\ln 2 - 3)/(5\pi) \approx 0.7317 \qquad \text{(uniform gas).} \tag{87}$$

As discussed above, within the RPA, all $\bar{C}^{(n)}$ vanish for $n \geq 3$.

We have also calculated this constant for Hooke's atom[**?**]. We use elementary perturbation theory, treating the Coulomb repulsion as weak. In the high density (non-interacting) limit, we find $\bar{C}^{(2)}$ in agreement with Eq. (81). We then calculate the leading corrections to $\bar{C}$, and find, after tedious calculations[65],

$$\alpha = 2 \; \ln[(2 + \sqrt{3})/8(2 - \sqrt{3})][5^{3/2}/(3^{11/6}\pi^{2/3})] \approx 0.7713 \qquad \text{(Hooke's atom).} \tag{88}$$

This result is a definitive counter-example to the short wavelength hypothesis. However, note that these values for α are not very much different numerically, suggesting that the short wavelength hypothesis may not be too bad in practice. (We have also found that, for the metal surface energy contribution in the semiclassical infinite barrier model, $\alpha = 0$ both exactly and in the LSD.)

Furthermore, we have calculated $C_{\lambda=1}$ both exactly and within the LSD for the ground state of the Hooke's atom at several finite densities. This is easily done for values of the frequency, ω, for which exact analytic solutions exist[10]. We find, for $\omega = 1/2$ ($r_s \geq 1.39$), $C_{\lambda=1} = 1.4904$ and $C_{\lambda=1}^{LSD} = 1.83$, making a 23% error. Since C is related to the zero separation hole through Eq. (80), this leads to an LSD error in $\langle n_{xc,\lambda=1}(\mathbf{0}) \rangle$ of only -4%. For comparison, the LSD errors[11] in the total exchange, correlation, and exchange-correlation energies are -14%,+124%, and -5%, respectively, and the corresponding PW91 errors[11] are -4%, +36%, and -1%. The relative LSD error in $C_{\lambda=1}$, which is purely correlation, is much smaller than that of the total correlation energy, as expected. LSD *is* almost exact for $g_{\lambda=1}(\mathbf{r}, \mathbf{r})$ at $r = 0$, where $\nabla n(\mathbf{r}) = 0$ and $g_{\lambda=1}(0, 0) = 0.2125$. This is reflected in the closeness of the two curves in Figure 6 at the origin, where the apparent difference may be due to errors in the parameterization of the LSD pair distribution function[33], rather than differences between the exact and LSD values.

Thus we have shown that the short wavelength hypothesis is not exact in general. Even if it were, it would not provide a strong explanation for the success of the local spin density approximation, because the k^{-6} tail of the exchange-correlation energy

is a small part of the total. We have also shown how earlier approximate arguments for the validity of the short wavelength hypothesis are limited to the high density regime. However, the specific cases studied all suggest that the short wavelength hypothesis is approximately true numerically. Away from the high-density, low-density, and fully spin-polarized limits, the reasons for the approximate validity of the short wavelength hypothesis remain, at best, intuitive, but this limited validity does help to justify generalized gradient approximations which revert to LSD for short wavelengths or small interelectronic separations.

4.4. Is the extended cusp condition universal?

Another possible universal condition on non-uniform electron gases is the extended electron-electron cusp condition. To state this condition precisely, we define the electron pair (or intracule) density in terms of the second-order density matrix, Eq. (14), as

$$I(\mathbf{u}) = \frac{1}{2} \int d^3r \ \rho_2(\mathbf{r}, \mathbf{r} + \mathbf{u}) \tag{89}$$

For simplicity, we work with the angle-average of the pair density

$$h(u) = \frac{1}{4\pi} \int d\Omega_u I(\mathbf{u}). \tag{90}$$

We observe that

$$\int_0^\infty du \ 4\pi u^2 h(u) = \frac{N(N-1)}{2} \tag{91}$$

is the number of distinct electron pairs, and that $4\pi u^2 h(u) \ du$ is the average number of pairs having interelectronic separation between u and $u+du$. Manifestly, $h(u) \geq 0$. Figure 18 displays $h(u)$ for the ground state of H^-. The radial intracule density $4\pi u^2 h(u)$ has recently proven useful in a study of the first-row hydrides[70].

In terms of $h(u)$, the zero-separation cusp condition, Eq. (31), is written as

$$h(0) = h'(0), \tag{92}$$

where $h'(u) \equiv dh(u)/du$. Recently, an extension of this cusp condition has been found to be true numerically, in a Hylleraas-type framework, for certain two-electron ions[71]. This extended cusp condition is simply stated as

$$h(u) - h'(u) \geq 0 \tag{93}$$

for all values of u. The above expression becomes an equality for $u = 0$, which corresponds to the usual cusp condition. This condition, along with the unimodality of $h(u)$[72], i.e., that $h(u)$ has only one extremum, has been used to generate exact bounds[73] on the central pair-density $h(0)$, the location u_{max} of the maximum of $h(u)$, and various expectation values $\langle u^\alpha \rangle$[71,72,74]. Other related results have been obtained by means of variational procedures[75] or from the study of the log-convexity of $h(u)$[76]. This naturally leads to the question of whether or not $h(u)$ obeys the extended cusp condition for the ground state of all electronic systems, the answer to which is the focus of this subsection.
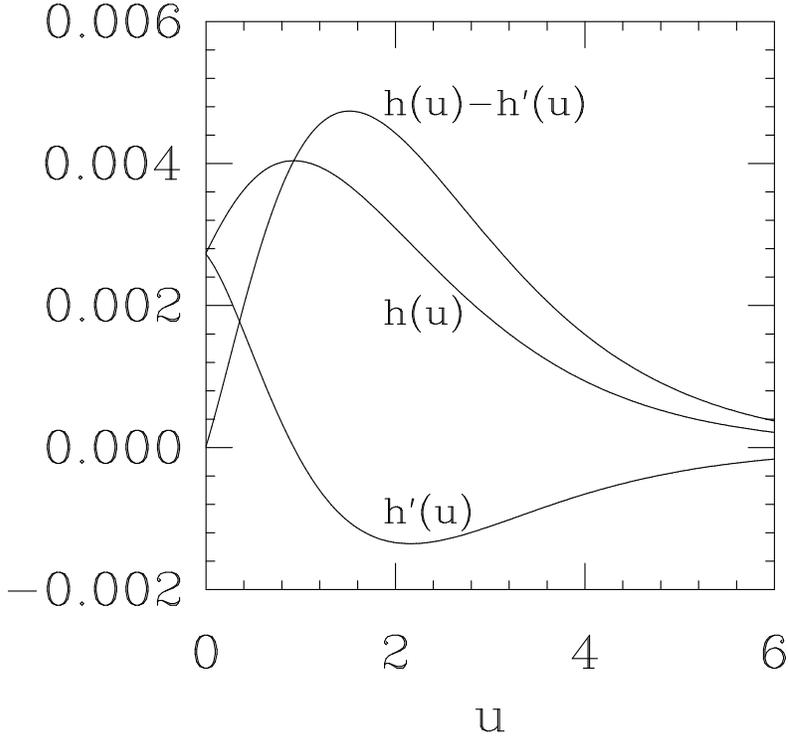
Figure 18. Electron pair density, $h(u)$, its radial derivative, $h'(u)$, and their difference, for H$^-$, calculated using a 204 term Hylleraas-type wavefunction, as described in Ref. [71].

We may also write $h(u)$ in terms of the pair distribution function for the system, $g(\mathbf{r}, \mathbf{r}')$, defined in Eq. (16),

$$h(u) = \frac{1}{2} \int d^3r \; n(\mathbf{r}) \int \frac{d\Omega_u}{4\pi} \; n(\mathbf{r} + \mathbf{u}) \; g(\mathbf{r}, \mathbf{r} + \mathbf{u}). \tag{94}$$

Note that there is no coupling-constant average here. For large values of u, $g(\mathbf{r}, \mathbf{r} + \mathbf{u}) \to 1$, so that $h(u)$ is typically a long-ranged function of u. We may separate out a reasonably short-ranged contribution, in the spirit of the LSD approximation. We write

$$h(u) = h_{sr}(u) + h_{lr}(u), \tag{95}$$

where

$$h_{sr}(u) = \frac{1}{2} \int d^3r \; n(\mathbf{r}) \int \frac{d\Omega_u}{4\pi} \; n_{xc}(\mathbf{r}, \mathbf{r} + \mathbf{u}) \tag{96}$$

and vanishes for large u, while

$$h_{lr}(u) = \frac{1}{2} \int d^3r \ n(\mathbf{r}) \int \frac{d\Omega_u}{4\pi} \ n(\mathbf{r} + \mathbf{u}). \tag{97}$$

Note that since $h_{lr}(u) = h_{lr}(0) + O(u^2)$ for small values of u, it has no cusp, and integrates to $N^2/2$, while $h_{sr}(u)$ contains the cusp, and integrates to $-N/2$. Now the expectation value of the electron-electron repulsion operator is

$$\langle \hat{V}_{ee} \rangle = \int_0^\infty du \ 4\pi u^2 \ h(u) \ \frac{1}{u}, \tag{98}$$

where the long-range (lr) part is the "direct classical Coulomb energy," treated exactly in Hartree, Hartree-Fock, and density functional theories[6], while the short-range (sr) part is amenable to a local spin density approximation, just like the exchange-correlation hole, as in Eq. (58).

In recent work, two of us (Burke and Perdew), with Juan Carlos Angulo[77] were able to prove analytically that this extended cusp condition was true for the ground state of Hooke's atom for *all* values of the spring constant. We also showed that $h(u)$ was always unimodal for this system, just as had been found for the two electron ions.

However, we also found, by explicit calculation, that the extended cusp condition was *violated* by the uniform electron gas of high density. To understand why, first note that, for a uniform system, Eq. (94) becomes

$$h(u) = \frac{1}{2} \ n \ N \ g(r_s, \zeta, u) \tag{99}$$

where n is the (uniform) density of the system, and $g(r_s, \zeta, u)$ is the pair distribution function in a uniform gas of density $n = 3/(4\pi r_s^3)$ and relative spin polarization ζ, at separation u. Now we separate $g(u)$ into its exchange and correlation contributions,

$$g(u) = g_x(u) + g_c(u). \tag{100}$$

In the high density limit, $g_x(u)$ dominates. Now $g_x(u)$ varies between $1/2$ and 1 on a length scale of order $1/(2k_F)$, and so $g_x'(u) \approx O(2k_F)$. We also know $g_x'(u)$ must be positive for some value of u. Thus, as $k_F \to \infty$, $g_x'(u)$ becomes very large and positive, while $g_x(u) \approx 1$, so that the extended cusp condition is violated. It is straightforward to check explicitly the well-known formula for $g_x(u)$ for the uniform gas[33] to see that it has these properties.

Note that such considerations do not apply to the cusp condition at the origin, which the uniform gas *does* obey. This is because $g_x(u)$ has no cusp at the origin, as stated in Eq. (32). Here the correlation contribution becomes significant, and in fact must suffice to fulfill the cusp condition. Since we know the behavior of $g(0)$ as $r_s \to 0$, Eq. (86), we deduce that, for $u \ll r_s \ll 1$,

$$g_c(u) = \frac{-\alpha r_s + u(1 - \alpha r_s)}{2} + O(u^2). \tag{101}$$

These two results suggest a possible contradiction. On the one hand, we showed that, at high densities, the uniform gas violates the extended cusp condition, and

gave a compelling argument for this result. However, in our paper[77], we also showed that the Hooke's atom obeys the extended cusp condition for all values of the spring force constant, including large values which produce a very high density. We next show that there is a qualitative difference between these two systems which explains why one violates the extended cusp condition, while the other does not.

Recall the separation of $h(u)$ into short- and long-ranged contributions. Consider how these separate contributions behave in the high-density limit of a two-electron system. Again, exchange dominates, but now $g_x(u) = 1/2$ everywhere. Thus we find, from Eqs. (94-97),

$$h(u) = \frac{1}{2}h_{lr}(u) = -h_{sr}(u). \tag{102}$$

Clearly, if $h(u)$ then obeys the extended cusp condition, so also does $h_{lr}(u)$; but $h_{sr}(u) - h'_{sr}(u) \leq 0$ for all u. In the particular case of the Hooke's atom, the high density (or non-interacting) limit is just a pair of three-dimensional harmonic oscillators. The ground state wavefunctions are simple Gaussians, yielding a density

$$n(r) = \frac{2}{u_o^3}\left(\frac{2}{\pi}\right)^{3/2} \exp(-2\,r^2/u_o^2), \tag{103}$$

where $u_o = (4/k)^{1/4}$ is a measure of the radius of the system. Eq. (97) then yields

$$h_{lr}(u) = \frac{2}{u_o^3}\left(\frac{1}{\pi}\right)^{3/2} \exp(-u^2/u_o^2). \tag{104}$$

Now, for u finite (and non-zero) on the scale of u_o, we find $h'_{lr}(u)/h_{lr}(0) \approx O(1/u_o)$, which becomes very large and negative for small u_o. But from Eq. (102), $h_{sr}(u) = -h_{lr}(u)/2$. Thus the extended cusp condition is obeyed by the total $h(u)$, but $h_{sr}(u)$ alone contains an extreme violation of the extended cusp condition.

To compare this high density behavior with that of the uniform gas, note that the short-range $h_{sr}(u)$ behaves quite similarly in both systems, while $h_{lr}(u)$ is very different. In fact, we can make an LSD approximation to $h_{sr}(u)$ for non-uniform systems, by defining

$$h_{sr}^{LSD}(u) = \frac{1}{2}\int d^3r\; n^2(\mathbf{r})\Big[g(r_s(\mathbf{r}), \zeta(\mathbf{r}), u) - 1\Big], \tag{105}$$

where $g(r_s(\mathbf{r}), \zeta(\mathbf{r}), u)$ is the uniform gas pair distribution function and $\zeta(\mathbf{r})$ is the relative spin polarization at r. In Fig. 19, we plot both $h_{sr}(u)$ and $h_{sr}^{LSD}(u)$ for the high density limit of the Hooke's atom, where the density is given by Eq. (103), $\zeta = 0$, $h_{sr}(u)$ is given by Eqs. (102) and (104), and g appearing in Eq. (105) contains only the exchange contribution. We see that the LSD approximation is generally good, especially in regions where $h_{sr}(u)$ is large. One of the reasons for its success is that $h_{sr}^{LSD}(u)$ integrates to -1, just as the exact $h_{sr}(u)$ does. Furthermore, for high densities, $g(r_s, \zeta = 0, u = 0) = 1/2$, so that $h_{sr}^{LSD}(u = 0) = h_{sr}(u = 0)$. At lower densities, the LSD value at the origin is expected to be approximately correct, as discussed in the previous subsection. Note that, while the decay in $h_{sr}(u)$ is due
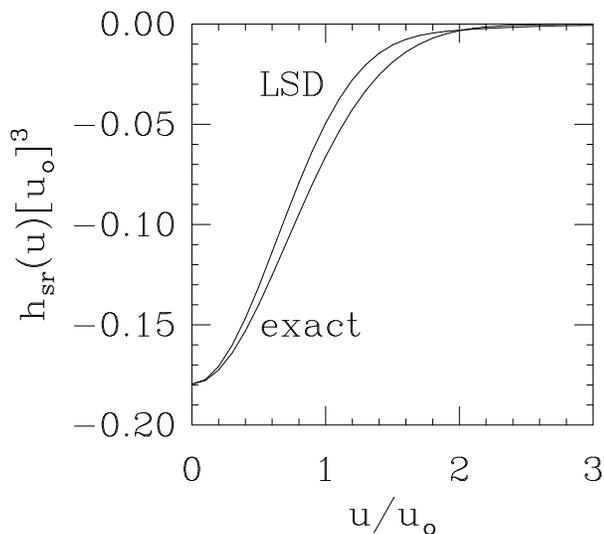
Figure 19. $h_{sr}(u)$ for the high-density limit of Hooke's atom.

entirely to the fall off in density of the Hooke's atom, as its pair distribution function $g = 1/2$ everywhere, the decay in $h_{sr}^{LSD}(u)$ is due to the decay in the uniform gas value of $g - 1$.

The above analysis explains why the uniform gas behaves so differently from the Hooke's atom in the high density limit. In both systems, $h_{sr}(u)$ behaves very similarly, developing a large, positive derivative for finite u as $n \to \infty$. However, the Hooke's atom $h'(u)$ also contains contributions from $h'_{lr}(u)$ due to the density gradient, which have no analog in the uniform electron gas. These are sufficient to cancel the contributions from $h'_{sr}(u)$, so that the extended cusp condition remains valid for this system.

Clearly, the most important conclusion from this work is that the extended cusp condition is not true for the ground state of all inhomogeneous systems. It may be true in more limited cases, e.g., for all two-electron systems, or perhaps for all atoms and ions. We can expect violations of the extended cusp condition in systems which have sufficiently large and slowly-varying densities. This is not the case for the high-density limit of few-electron ions, where the density never becomes nearly uniform. For the Hooke's atom discussed here, Eq. (103) shows that the density always varies on the length scale u_o, the "radius" of the atom. This example illustrates the danger of assuming that conditions which are obeyed by specific classes of systems can be transferred to all inhomogeneous electron systems.

5. APPLICATIONS OF GGA's

In this section we give a brief (not comprehensive) survey of some results which have been reported using GGA's. While the detailed numbers for a given calculation vary when the different GGA's are used, the overall trends, concerning which quantities are improved by a good GGA relative to LSD, typically do not. However, since the PW91 form is derived from first principles (essentially without semi-empirical parameters) and obeys more exact conditions than any of the others, as discussed in section 3.2, we strongly recommend it for future calculations. The codes are freely available on request to John Perdew (perdew@mailhost.tcs.tulane.edu).

5.1. Atoms

Table 1 gives the exchange energy for He and Ne (Hartree-Fock densities) and for the Hooke's atom within the LSD approximation, the PW91 GGA, and exactly. For the Hooke's atom, we consider two different spring constants, $k = 0.25$ ($r_s > 1.39$), for which the density was plotted in Figure 1, and $k = 3.6 \times 10^{-6}$ ($r_s > 44.3$). We see that LSD recovers only about 90% of the total exchange energy of a real atom. Comparison of the $r_s = 0$ curves of Figures 7 and 14 explains why LSD underbinds

Table 1
Exchange energies of atoms (eV)

atom	LSD	GEA	PW91	Exact
He	-24.06	-27.39	-27.67	-27.91
Ne	-300.22	-320.39	-329.65	-329.49
Hooke's (high spring constant)	-12.00		-13.43	-14.02
Hooke's (low spring constant)	-0.47		-0.53	-0.53

The real atom results are from Ref.[78]; the Hooke's atom results are from Ref.[11].

electrons. LSD, by ignoring the density gradient, misses a substantial fraction of the exchange energy. The numerical PW91 reduces the error to the level of 1% or less; even smaller errors are found with the analytic PW91 (slightly biased because it is based upon a modification of the Becke form, which was fitted to exact exchange energies of atoms). Note that PW91 does well, not only for real atoms, but also for Hooke's atom.

Table 2 is the same as Table 1, but reports correlation energies. LSD overestimates the magnitudes of the correlation energies of atoms by about a factor of two. This can be understood from the $r_s \neq 0$ curves of Figures 7 and 14. For large s the curves of Figure 14 all approach the $r_s = 0$ curve, showing that correlation turns off for high gradients. Clearly, LSD does not account for this feature. Note that this correction is achieved in PW91 *without fitting to known energies*, and that the GEA correlation energies even have the wrong sign. Again, PW91 does better than LSD, but the improvement over LSD is not as dramatic for the Hooke's atom as for real atoms. Both exchange and correlation energies were found to be improved by

Table 2
Correlation energies of atoms (eV)

atom	LSD	GEA	PW91	Exact
He	−3.06	3.40	−1.25	−1.14
Ne	−20.21	21.23	−10.41	−10.61
Hooke's (high spring constant)	−2.35		−1.43	−1.05
Hooke's (low spring constant)	−0.29		−0.23	−0.17

The real atom results are from Ref.[78]; the Hooke's atom results are from Ref.[11].

several GGA's for six noble gas atoms[79].

Table 3 reports the total exchange-correlation energies for the atoms listed in Table 1. We see the well-known cancellation of error between exchange and cor-

Table 3
Exchange-correlation energies of atoms (eV)

atom	LSD	GEA	PW91	Exact
He	−27.12	−23.99	−28.92	−29.05
Ne	−320.43	−299.16	−340.06	−340.04
Hooke's (high spring constant)	−14.35		−14.86	−15.07
Hooke's (low spring constant)	−0.76		−0.76	−0.70

The real atom results are from Ref.[78]; the Hooke's atom results are from Ref.[11].

relation in LSD, which is also present in PW91. We believe that this cancellation can at least in part be attributed to the cancellation of the long-range parts of the exchange and correlation holes in these approximations, which is probably present in the exact hole, as discussed in section 2.4. To retain this property, one should avoid mixing different approximations to exchange and correlation.

We also list some results for ionization energies and electron affinities, computed from the differences of ion and neutral atom total energies, in Table 4. The Hartree-Fock (HF) approximation seriously underestimates these quantities. For some of the cases shown, PW91 in fact does slightly worse than LSD for these quantities, and, looked at over the entire periodic table, shows no systematic improvement on the LSD approximation. The interconfigurational energy error of LSD, which overbinds d electrons relative to p, and p relative to s, persists; both LSD and PW91 are most accurate for "term-conserving s processes," in which two or more s-electrons are removed with no change of total angular momentum or spin[43]. The exchange-correlation potential $v_{xc}(r)$ is also improved at best marginally[80,11]: PW91 picks up the intershell bumps that are missing in LSD, but does not improve the $r \to \infty$ behavior in an atom, and worsens the $r \to 0$ behavior of the potential. Fortunately, these defects do not substantially affect the total energy. We did not

Table 4
Electron removal energies of atoms

	Ionization Energy (eV)				Electron Affinity (eV)			
atom	HF	LSD	PW91	Expt.	HF	LSD	PW91	Expt.
H	13.61	13.00	13.63	13.61	-0.33	0.91	0.71	0.75
Li	5.34	5.45	5.61	5.39	-0.12	0.58	0.53	0.62
C	10.78	11.67	11.64	11.26	0.55	1.67	1.63	1.26
O	11.88	13.82	13.76	13.62	-0.54	1.93	1.74	1.46

All results are from Ref.[43].

include these conditions in our discussion in section 2, since these are conditions which are not shared by all inhomogeneous Coulomb-interacting systems.

5.2. Molecules

With a few exceptions discussed below, the LSD approximation tends to produce good structure for many molecules, so that bond lengths, bond angles, dipole moments, and vibrational frequencies are typically good to within a few percent[81–88]. PW91 does equally well, with perhaps a marginal improvement, for these quantities. For small molecules composed of the elements H, C, N, O, and F, Andzelm and Wimmer[83] find, using BP, bond length errors of about 0.02Å, bond angle errors of only $1 - 2°$, and vibrational frequencies to within 3-5%, which were as good as those found with several wavefunction methods, and much better than HF. Kutzler and Painter[84] find that GGA bond lengths and frequencies are not much improved over LSD in first row diatomic molecules.

An important corollary of these results is that it seems one may often optimize the geometry and electron density of a molecule within the LSD approximation, and only then look at the energy changes produced by the GGA functional, i.e., not self-consistently, with little further error[81,89,88].

Atomization and dissociation energies of molecules are typically underestimated by the Hartree-Fock (HF) approximation (especially for molecules with nearly-degenerate Hartree-Fock ground states), and overestimated by the LSD approximation. The LSD underbinding of electrons produces a greater error in the fragments of a molecule than in the whole. Because PW91 cures the underbinding problem, it reduces the LSD error by a factor of about five, from about 1 eV per bond to about 0.2 eV per bond, as shown by the examples listed in Table 5.

These kinds of improvements have been seen in almost all molecules studied to date: in early calculations on O_2, Mg_2, CH_2, using PW86[92]; for the HCNOF molecules using both BP[83] and PW86[93]; for a large variety using BLYP[85]; for some pseudopotential calculations[86]; for the traditionally-difficult molecules[94] O_3, S_3, CH_2, and Be_2 using BP and BLYP; for neutral N_xO_y molecules using BP[88]; and for the first row dimers[84] and hydrides[95].

Becke has shown[82] that much of this improvement comes from the improved treatment of exchange. In fact, just applying his gradient correction for exchange, and still treating correlation within the LSD approximation, often does a little

Table 5
Atomization energies of molecules (eV)

molecule	HF	LSD	PW91	Expt.
C_2	0.73	7.51	6.55	6.36
C_6H_6	45.19	68.42	61.34	59.67
H_2	3.29	4.65	4.52	4.49
H_2O	5.71	11.00	9.59	9.51
O_2	1.25	7.48	5.93	5.12

Results for the carbon-based molecules are from Ref.[43], and
omit the zero point energy; the other results include the zero
point energy, and for these other molecules PW91 and Expt.
are from Ref.[90], HF from Ref.[85], and LSD from Ref.[91].

better than, say, PW91[82,95,84]. However, such a treatment lacks theoretical
justification, and fails dramatically for the metallic surface energy[43]. It also
leads, for example, to worse ionization potentials than even LSD[82,95], and we
strongly advise against its use.

An alternative approach starts from the HF method and adds a gradient-corrected
density functional for the correlation energy[96,97], which reduces the severity of
the HF underbinding of molecules. Fuentealba et al.[96] have found that the
Wilson-Levy correlation functional provides a more realistic correction to HF disso-
ciation energies than does even PW91. However, results still closer to experiment
(especially for molecules like C_2 and O_2) are found by taking *both* exchange and
correlation within GGA, as in Table 5, presumably for the reasons discussed at the
end of section 5.1.

An important situation in which LSD is insufficient, even for structure, is hy-
drogen bonding. Table 6 gives results for the O-O equilibrium distance and the
dissociation energy of the water dimer [$\equiv 2\times$(energy of H_2O) - (energy of $(H_2O)_2$)].
Similar results have been found in other studies with BP[99] and with PW91[90],

Table 6
Equilibrium properties of water dimer

property	LSD	BP	HF+MP2	Expt.
d(O-O) (Å)	2.72	2.93	2.91	2.98
E_{dimer} (eV)	0.36	0.18	0.23	0.21

From Ref.[98].

and also in studies of the high pressure phases of ice[100]. Another example is
provided by metal-ligand complexes[81], in which it appears that bond distances
depend strongly on electron correlation. LSD underestimates metal-ligand bond
lengths by about 0.05 Å, while BP reduces this error to 0.01 Å. Lastly along these
lines, we note a molecule for which even GGA's have difficulty[101]. The bond en-
ergy of the NF bond in FNO is overestimated by about 2 eV in LSD, and the bond

length underestimated by 0.03 Å. Both BP and BLYP reduce the error, but only to about 1 eV, and unfortunately overestimate the bond length by 0.05 Å.

The energies of chemical transition states are similarly improved by GGA. BP was found to be as good as HF for the energies of transition states in several model organic and organometallic reactions[102]. Barrier heights in LSD appear always to be seriously underestimated. Similar results were found using BP, BLYP, and PW91, for silylene insertion reactions into H_2[87].

While GGA often reduces the LSD error in chemical bond energies by about a factor of five, *another* factor-of-five improvement is needed to achieve the "chemical accuracy" with which nearly all chemical reactions could be predicted reliably.

5.3. Clusters and surfaces

For small clusters, the literature suggests the same trends as for molecules: geometries are typically not changed by the addition of gradient corrections, but cohesive energies are lowered. This has been seen for small clusters of Ni[92], Ag[103], As and P[104], and Mg[105]. Again, a notable exception is provided by the failure of LSD to correctly describe hydrogen bonding in H_2O. Structures of small water clusters, using the BP functional and the Vanderbilt ultrasoft oxygen pseudopotentials[106], were found[107] in good agreement with existing HF calculations.

In the study of small Ni clusters mentioned above[92], chemisorption energies were calculated for H on Ni_4 as a model for the chemisorption of H on the Ni(111) surface, and for H on Ni_5, as a model for H/Ni(100). The results are given in Table 7.

Table 7
Chemisorption energies of H on Ni clusters

cluster	LSD	PW86	Surface Expt.
Ni_4H	4.59	2.77	2.73
Ni_5H	3.59	2.91	2.73

From Ref.[92].

Again, just as in molecular studies, the barrier for dissociative adsorption of H_2 on Al(100) was found to be 0.54 eV/molecule using PW91, as compared with the LSD value of 0.25 eV/molecule[108]. In this case, the geometry of the transition state is well-described by the LSD.

Finally, the metal surface energy or surface tension will be discussed. Although the experimental values are uncertain, the surface energy is known exactly within the random phase approximation (RPA) for the infinite barrier model of the jellium surface[62,109,12]. RPA versions of LSD and PW91 have been tested[43] against this exact solution. While PW91 greatly improves upon LSD for the separate exchange and correlation components, the sum is slightly worsened, being underestimated more by PW91 than by LSD.

5.4. Solids

Bulk solids typically have well-bounded values of the reduced density gradient s, and so might be particularly amenable to GGA description. However, the full verdict is not yet in. We emphasize here the importance of performing full-potential all-electron calculations in tests of GGA's, and avoiding as much as possible further approximations, such as pseudopotential or shape approximations, which may lead to errors which mask the effects of the GGA, relative to LSD.

PW91 appears to improve the properties of both simple[43,110] and transition metals[111]. For example, LSD tends to underestimate bond lengths of molecules and solids, including metals. Even in the alkali metals Li and Na, which are often compared with the uniform electron gas, this error is about 4%. PW91 expands the lattice, producing lattice constants in better agreement with experiment, as seen in Table 8. GGA's also improve cohesive energies, just as they improve atomization en-

Table 8
Properties of solid metals

metal	Lattice constant (bohr)			Bulk modulus (GPa)		
	LSD	PW91	Expt.	LSD	PW91	Expt.
Li(bcc)	6.36	6.51	6.57	15.0	13.4	13.0
Na(bcc)	7.65	7.97	7.98	9.2	7.1	7.4
V(bcc)	5.53	5.66	5.74	212	184	157
Nb(bcc)	6.14	6.25	6.24	189	167	170

Li and Na results are from Ref.[43]; V and Nb results are from Ref.[111].

ergies in molecules. Earlier results, employing the atomic spheres approximation, which apparently showed that the GGA did not improve on LSD for Nb and Pd[112] and all $4d$ and $5d$ transition metals[113,114], were later shown to be insufficiently accurate to show the marked improvement due to the GGA[111].

Results for semiconductors may depend upon the chosen pseudopotential[115, 112,110,116]. Table 9 summarizes some results, listing them by how the pseudopotential for the core electrons was constructed, and how the valence electrons were treated. The considerable variation in these results suggests that more all-electron calculations may be needed to decide this issue. Trends suggest that, in going from LSD to GGA, the lattice constant, a, goes from underestimated to overestimated, the cohesive energy, E_{coh}, is improved, but the bulk modulus, B, is worsened.

Many transition-metal oxides and fluorides are insulators which LSD incorrectly describes as metals[119]. For some of these materials, full-potential GGA calculations open up a small fundamental gap which LSD misses, and so correct the description. For others, GGA enhances the gap, and generally improves the energy bands[119]. Of course, the sizes of the band-structure gaps are not physically meaningful in LSD, GGA, or even with the exact Kohn-Sham potential for the neutral solid. To get a physically meaningful fundamental gap, one must take account

Table 9
Properties of solid Si in various calculations

core-valence	$a(\text{Å})$	$\text{E}_{coh}(\text{eV})$	$B(\text{GPa})$
Expt.	5.43	4.63	98.8
LSD-LSD[115]	5.37	5.35	
LSD-LSD[112]	5.37	5.37	98
LSD-LSD[110]	5.38	5.38	96.6
LSD-LSD[116]	5.40		96.0
LSD (all-electron)[117]	5.43	5.25	95
LSD (all-electron)[118]	5.40	5.27	103
LSD-BP[112]	5.39	4.64	94
BP-BP[115]	5.49	4.41	
BP-BP[112]	5.47	4.50	88
BP-BP[116]	5.49		88.0
PW91-PW91[110]	5.59	4.64	85.2
BPW91 (all-electron)[118]	5.47	4.29	92

of the discontinuity[40,41] in the exact potential due to the addition of one electron to the infinite neutral solid.

Concerning magnetic properties, the LSD ground state for Fe is fcc nonmagnetic, but the GGA ground state is correctly bcc ferromagnetic[120,121]. GGA antiferromagnetic moments are more realistic than those of LSD for the transition-metal oxides[119], but results for the transition metals V, Cr, and Pd, are mixed[122].

6. CONCLUDING REMARKS AND PROSPECTS

We have shown how GGA's are constructed from exact conditions which all electronic systems are known to obey. These include conditions on the exchange-correlation hole itself, and scaling relations for the exchange-correlation energy. We have also seen some of the limitations of GGA's: their failure for large reduced density gradients, the challenge posed by the low-density convexity constraint, the behavior of the exchange-correlation hole at zero separation, etc.

A possible rationale for the successes and failures of GGA is this: GGA improves the short- to intermediate-range behavior of the exchange-correlation hole in comparison with LSD, and cuts off the long-range behavior. In small systems (atoms, molecules), the exact exchange-correlation hole cannot be long-ranged, since it is cut off by the exponential decay of the electron density into the vacuum in all three dimensions, so GGA is almost-always superior to LSD. But in large systems (bulk solids, surfaces), the exact hole can have a long-range tail. For example, the hole falls off like u^{-5} in the bulk of jellium, and like u^{-4} around an electron at the jellium surface. By missing this tail, GGA may underestimate the positive exchange-correlation contribution σ_{xc} to the surface energy.

LSD and GGA should best describe those properties of an electronic system that depend upon the short-range parts of the exchange or correlation holes. An

example is provided by the noninteracting kinetic energy $T_s[n_\uparrow, n_\downarrow]$, the first term on the right of Eq. (4). Because of the great importance and simplicity of this term, it is treated exactly in the Kohn-Sham scheme of section 1.1. However, if one approximates this term by a semilocal functional, one finds that its GEA is its own GGA[123]. Other short-range properties are the antiparallel-spin correlation energy and the correction to the random phase approximation[124]. To achieve much greater accuracy in electronic structure calculations, the exchange energy and the long-range part of the correlation energy might need to be treated exactly, or at least in a fully-nonlocal way, leaving only the short-range part of the correlation energy to be approximated via GGA[124].

REFERENCES

1. Peter Fulde, *Electron Correlations in Molecules and Solids* (Springer-Verlag, Berlin, 1991).
2. P. Hohenberg and W. Kohn, Phys. Rev. **136**, B 864 (1964).
3. M. Levy, Proc. Natl. Acad. Sci. (U.S.A.) **76**, 6062 (1979).
4. M. Levy, Phys. Rev. A **26**, 1200 (1982).
5. E. H. Lieb, Int. J. Quantum Chem. 24, 224 (1983).
6. W. Kohn and L.J. Sham, Phys. Rev. **140**, A 1133 (1965).
7. E. K. U. Gross and W. Kohn, in *Advances in Quantum Chemistry, vol. 21: Density Functional Theory of Many-Fermion Systems*, edited by S. B. Trickey (Academic Press, San Diego, 1990).
8. P. M. Laufer and J. B. Krieger, Phys. Rev. A **33**, 1480 (1986).
9. S. Kais, D. R. Herschbach, N. C. Handy, C. W. Murray, and G. J. Laming, J. Chem. Phys. 99, 417 (1993).
10. M. Taut, Phys. Rev. A 48, 3561 (1993).
11. C. Filippi, C. J. Umrigar, and M. Taut, J. Chem. Phys. **100**, 1290 (1994).
12. D.C. Langreth and J.P. Perdew, Phys. Rev. B **15**, 2884 (1977).
13. R.G. Parr and W. Yang, *Density Functional Theory of Atoms and Molecules* (Oxford, New York, 1989).
14. R.M. Dreizler and E.K.U. Gross, *Density Functional Theory* (Springer-Verlag, Berlin, 1990).
15. J. C. Kimball, Phys. Rev. A **7**, 1648 (1973).
16. E. R. Davidson, *Reduced Density Matrices in Quantum Chemistry*, (Academic Press, New York, 1976).
17. H. K. Schweng, H. M. Böhm, A. Schinner, and W. Macke, Phys. Rev. B 44, 13291 (1991).
18. K. Burke, J. P. Perdew, D. C. Langreth, Phys. Rev. Lett. **73**, 1283 (1994).
19. M. Levy and J.P. Perdew, Phys. Rev. A **32**, 2010 (1985).
20. M. Levy, Int. J. Quantum Chem. s**23**, 617 (1989).
21. M. Levy, Phys. Rev. A 43, 4637 (1991).

22. A. Görling and M. Levy, Phys. Rev. A **45**, 1509 (1992).
23. A. Görling, M. Levy, and J.P. Perdew, Phys. Rev. B **47**, 1167 (1993).
24. M. Levy and J. P. Perdew, Phys. Rev. B **48**, 11638 (1993).
25. M. Levy, Bull. Amer. Phys. Soc. **39**, 671 (1994).
26. M. Levy, in *Density Functional Theory*, eds. R. Dreizler and E. K. U. Gross, NATO ASI Series (Plenum, New York, 1994), to appear.
27. E. H. Lieb and S. Oxford, Int. J. Quantum Chem. **19**, 427 (1981).
28. J.P. Perdew, in *Electronic Structure of Solids '91*, edited by P. Ziesche and H. Eschrig (Akademie Verlag, Berlin, 1991).
29. D. M. Ceperley and B. J. Alder, Phys. Rev. Lett. **45**, 566 (1980).
30. W. E. Pickett and J. Q. Broughton, Phys. Rev. B **48**, 14859 (1993).
31. S. H. Vosko, L. Wilk, and M. Nusair, Can. J. Phys. **58**, 1200 (1980).
32. J. P. Perdew and Y. Wang, Phys. Rev. B **45**, 13244 (1992).
33. J. P. Perdew and Y. Wang, Phys. Rev. B **46**, 12947 (1992).
34. J. He and J. P. Perdew, unpublished.
35. O. Gunnarsson, M. Jonson, and B. I. Lundqvist, Phys. Rev. B **20**, 3136 (1979).
36. O. Gunnarsson and B.I. Lundqvist, Phys. Rev. B **13**, 4274 (1976).
37. J. P. Perdew and A. Zunger, Phys. Rev. B **23**, 5048 (1981).
38. J. P. Perdew and M. Levy, in *Many-Body Phenomena at Surfaces*, eds. D. C. Langreth and H. Suhl (Academic, New York, 1984).
39. J.P. Perdew, R.G. Parr, M. Levy, and J.L. Balduz, Jr., Phys. Rev. Lett. **49**, 1691 (1982).
40. J. P. Perdew and M. Levy, Phys. Rev. Lett. **51**, 1884 (1983).
41. L. J. Sham and M. Schlüter, Phys. Rev. Lett. **51**, 1888 (1983).
42. J. B. Krieger, Y. Li, and G. J. Iafrate, in *Density Functional Theory*, eds. R. Dreizler and E. K. U. Gross, NATO ASI Series (Plenum, New York, 1994), to appear.
43. J. P. Perdew, J. A. Chevary, S. H. Vosko, K. A. Jackson, M. R. Pederson, D.J. Singh, and C. Fiolhais, Phys. Rev. B **46**, 6671 (1992); **48**, 4978 (1993) (E).
44. M. Rasolt and H.L. Davis, Phys. Lett. A **86**, 45 (1981).
45. M. Rasolt and D.J.W. Geldart, Phys. Rev. B **34**, 1325 (1986).
46. D.C. Langreth and J.P. Perdew, Phys. Rev. B **21**, 5469 (1980).
47. J.P. Perdew, Phys. Rev. Lett. **55**, 1665 (1985); **55**, 2370 (1985) (E).
48. S.-K. Ma and K.A. Brueckner, Phys. Rev. **165**, 18 (1968).
49. D.C. Langreth and M.J. Mehl, Phys. Rev. B **28**, 1809 (1983).
50. C.D. Hu and D.C. Langreth, Phys. Scr. **32**, 391 (1985).
51. J.P. Perdew, Phys. Rev. B **33**, 8822 (1986); **34**, 7406 (1986) (E).
52. J.P. Perdew and Y. Wang, Phys. Rev. B **33**, 8800 (1986); **40**, 3399 (1989) (E).
53. A.D. Becke, Phys. Rev. A **38**, 3098 (1988).
54. C. Lee, W. Yang, and R.G. Parr, Phys. Rev. B **37**, 785 (1988).
55. B. Miehlich, A. Savin, H. Stoll, and H. Preuss, Chem. Phys. Lett. **157**, 200 (1989).
56. C. Umrigar and X. Gonze, proceedings of the *Conference on Concurrent Computing in the Physical Sciences, 1993*, to be published.
57. L. C. Wilson and M. Levy, Phys. Rev. B **41**, 12930 (1990).

58. J.P. Perdew, Physica B **172**, 1 (1991).
59. J. P. Perdew, K. Burke, and Y. Wang, unpublished.
60. E. Engel, J.A. Chevary, L.D. MacDonald, and S.H. Vosko, Z. Phys. D **23**, 7 (1992).
61. D.J. Lacks and R.G. Gordon, Phys. Rev. A **47**, 4681 (1993).
62. D.C. Langreth and J.P. Perdew, Solid State Commun. **17**, 1425 (1975).
63. D. C. Langreth and J. P. Perdew, Solid State Commun. **31**, 567 (1979).
64. D.C. Langreth and J.P. Perdew, Phys. Lett. A **92**, 451 (1982).
65. K. Burke and J.P. Perdew, unpublished.
66. H. Yasuhara, Solid State Commun. **11**, 1481 (1972).
67. D. M. Ceperley, Phys. Rev. B **18**, 3126 (1978)
68. D. J. W. Geldart, Can. J. Phys. **45**, 3139 (1967).
69. J. C. Kimball, Phys. Rev. B **14**, 2371 (1976).
70. J. Wang and V. H. Smith, Jr., Int. J. Quantum Chem. **49** 147 (1994).
71. J. S. Dehesa, J. C. Angulo, T. Koga and K. Matsui, Z. Phys. D **25**, 9 (1992).
72. J. S. Dehesa, J. C. Angulo and T. Koga, Z. Phys. D **25**, 3 (1992).
73. J. S. Dehesa, J. C. Angulo, T. Koga and K. Matsui, Phys. Rev. A **47**, 5202 (1993).
74. J. S. Dehesa, J. C. Angulo, T. Koga and Y. Kasai, Phys. Rev. A **48**, 832 (1993).
75. T. Koga, Y. Kasai, J. S. Dehesa and J. C. Angulo, Phys. Rev. A **48**, 2457 (1993).
76. J. S. Dehesa, J. C. Angulo, T. Koga and Y. Kasai, accepted in Phys. Rev. A.
77. K. Burke, J. C. Angulo, and J. P. Perdew, Phys. Rev. A **50**, 297 (1994).
78. J.P. Perdew, in *Many-Body Physics*, edited by J.N. Urbano, C. Fiolhais, M. Fiolhais, and C. Sousa (World Scientific, Singapore, 1994).
79. T. Zhu, C. Lee, and W. Yang, J. Chem. Phys. **98**, 4814 (1993).
80. E. Engel and S.H. Vosko, Phys. Rev. B **47**, 13164 (1993).
81. L. Fan and T. Ziegler, J. Chem. Phys. **95**, 7401 (1991).
82. A.D. Becke, J. Chem. Phys. **96**, 2155 (1992).
83. J. Andzelm and E. Wimmer, J. Chem. Phys. **96**, 1280 (1992).
84. F. W. Kutzler and G. S. Painter, Phys. Rev. B **45**, 3236 (1992).
85. B. G. Johnson, P. M. W. Gill, J. A. Pople, J. Chem. Phys. **98**, 5612 (1993).
86. H. Chen, M. Krasowski, and G. Fitzgerald, J. Chem. Phys. **98**, 8710 (1993).
87. C. Sosa and C. Lee, J. Chem. Phys. **98**, 8004 (1993).
88. A. Stirling, I. Pápai, J. Mink, and D. R. Salahub, J. Chem. Phys. **100**, 2910 (1994).
89. C. Lee, G. Fitzgerald, and W. Yang, J. Chem. Phys. **98**, 2971 (1993).
90. J. M. Seminario, to appear in Int. J. Quantum Chem. S **28** (1994).
91. A.D. Becke, J. Chem. Phys. **97**, 9173 (1992).
92. P. Mlynarski and D.R. Salahub, J. Chem. Phys. **95**, 6050 (1991)
93. J. M. Seminario, Chem. Phys. Lett. **206**, 547 (1993).
94. C. W. Murray, N. C. Handy, and R. D. Amos, J. Chem. Phys. **98**, 7145 (1993).
95. R. Merkle, A. Savin, and H. Preuss, Chem. Phys. Lett. **194**, 32 (1992).
96. P. Fuentealba and A. Savin, Chem. Phys. Lett. **217**, 566 (1994).
97. M. Causá and A. Zupan, Chem. Phys. Letters **220**, 145 (1994).
98. K. Laasonen, F. Csajka, and M. Parinello, Chem. Phys. Lett. **194**, 172 (1992).
99. R. N. Barnett and U. Landman, Phys. Rev. Lett. **70**, 1775 (1993).
100. C. Lee, D. Vanderbilt, K. Laasonen, R. Car, and M. Parrinello, Phys. Rev. Lett.

69, 462 (1992).

101. T. S. Dibble, J. S. Francisco, R. J. Deeth, M. R. Hand, and I. H. Williams, J. Chem. Phys. **100**, 459 (1994).

102. R. V. Stanton and K. M. Merz, J. Chem. Phys. **100**, 434 (1994).

103. R. Santamaria, I. G. Kaplan, and O. Novaro, Chem. Phys. Lett. **218**, 395 (1994).

104. P. Ballone and R.O. Jones, J. Chem. Phys. **100**, 4941 (1994).

105. P. Delaly, P. Ballone, and J. Buttet, Phys. Rev. B **45**, 3838 (1992).

106. D. Vanderbilt, Phys. Rev. B **41** , 7892 (1990).

107. K. Laasonen, M. Parrinello, R. Car, C. Lee, and D. Vanderbilt, Chem. Phys. Lett. **207**, 208 (1993).

108. B. Hammer, K.W. Jacobsen, and J.K. Nørskov, Phys. Rev. Lett. **70**, 3971 (1993).

109. E. Wikborg and J.E. Inglesfield, Solid State Commun. **16**, 335 (1975).

110. Y.-M. Juan and E. Kaxiras, Phys. Rev. B **48**, 14944 (1993).

111. V. Ozolins and M. Körling, Phys. Rev. B **48**, 18304 (1993).

112. A. Garcia, C. Elsässer, J. Zhu, S.G. Louie, and M.L. Cohen, Phys. Rev. B **46**, 9829 (1992); **47**, 4130 (1993) (E).

113. B. Barbiellini, E.G. Moroni, and T. Jarlborg, J. Phys. Condens. Matter **2**, 7597 (1990).

114. M. Körling and J. Haglund, Phys. Rev. B **45**, 13293 (1992).

115. G. Ortiz, Phys. Rev. B **45**, 11328 (1992).

116. A. Dal Corso, S. Baroni, and R. Resta, Phys. Rev. B **49**, 5323 (1993).

117. G. te Velde and E. J. Baerends, Phys. Rev. B **44**, 7888 (1991).

118. M. Causá and A. Zupan, to appear in Int. J. Quantum Chem. (1994) and private communication.

119. P. Dufek, P. Blaha, V. Sliwko, and K. Schwarz, Phys. Rev. B **49**, 10170 (1994).

120. P. Bagno, O. Jepsen, and O. Gunnarsson, Phys. Rev. B **40**, 1997 (1989).

121. C. Amador, W.R.L. Lambrecht, and B. Segall, Phys. Rev. B **46**, 1870 (1992).

122. D. J. Singh and J. Ashkenazi, Phys. Rev. B **46**, 11570 (1992).

123. J.P. Perdew, Phys. Lett. A **165**, 79 (1992).

124. J.P. Perdew, Int. J. Quantum Chem. S **27**, 93 (1993).